Steel and Composite Structures, *Vol. 18, No. 1 (2015) 91-120*
DOI: http://dx.doi.org/10.12989/scs.2015.18.1.091

A refined higher-order shear deformation theory for bending, vibration and buckling analysis of functionally graded sandwich plates

Kien T. Nguyen [*1], Tai H. Thai [2] and Thuc P. Vo [3]

[1] *Faculty of Civil Engineering and Applied Mechanics, University of Technical Education, Ho Chi Minh City, 1 Vo Van Ngan Street, Thu Duc District, Ho Chi Minh City, Viet Nam*
[2] *School of Civil and Environmental Engineering, The University of New South Wales, NSW 2052, Australia*
[3] *Faculty of Engineering and Environment, Northumbria University, Newcastle upon Tyne, NE1 8ST, UK*

(*Received December 26, 2013, Revised April 28, 2014, Accepted May 27, 2014*)

Abstract. A refined higher-order shear deformation theory for bending, vibration and buckling analysis of functionally graded sandwich plates is presented in this paper. It contains only four unknowns, accounts for a hyperbolic distribution of transverse shear stress and satisfies the traction free boundary conditions. Equations of motion are derived from Hamilton's principle. The Navier-type and finite element solutions are derived for plate with simply-supported and various boundary conditions, respectively. Numerical examples are presented for functionally graded sandwich plates with homogeneous hardcore and softcore to verify the validity of the developed theory. It is observed that the present theory with four unknowns predicts the response accurately and efficiently.

Keywords: functionally graded sandwich plates; bending; buckling; vibration

1. Introduction

Functionally graded (FG) sandwich structures are advanced composite materials that have smooth variations of material properties to eliminate the stress concentrations at the interfaces between faces and core found in conventional sandwich structures. These advanced structures are recently developed for various engineering applications where strong stiff and light structures are required. Typically, the FG sandwich plate faces are made from a mixture of ceramic and metal constituents which are continuously varied while the core is fully homogeneous material.

Increase of FG material applications in engineering structures has led to the development of many plate theories to predict accurately the bending, buckling and vibration behaviours of FG plates. The classical plate theory (CPT) (Feldman and Aboudi 1997, Javaheri and Eslami 2002, Mahdavian 2009, Mohammadi *et al*. 2010, Chen *et al*. 2006, Baferani *et al*. 2011) yields acceptable results only for the thin plates, whereas accuracy of the first-order shear deformation theory (FSDT) (Mohammadi *et al*. 2010, Croce and Venini 2004, Efraim and Eisenberger 2007,

*Corresponding author, Ph.D. Kien T. Nguyen, E-mail: kiennt@hcmute.edu.vn

http://www.techno-press.org/?journal=scs&subpage=8 ISSN: 1229-9367 (Print), 1598-6233 (Online)

Zhao *et al*. 2009a, b, Lee *et al*. 2009, Hosseini-Hashemi *et al*. 2011, Naderi and Saidi 2010, Nguyen-Xuan *et al*. 2012, Thai and Choi 2013a) depends on the shear correction factor. Higher-order shear deformation theories with five unknown functions, which are included third-order shear deformation plate theory (TSDT), sinusoidal shear deformation plate theory (SSDT), hyperbolic shear deformable plate theory (HSDT), exponential shear deformation plate theory (ESDT), predict more accurate the response of moderate and thick FG plates (Reddy 2000, Zenkour 2006, Matsunaga 2008, Chen *et al*. 2009, Pradyumna and Bandyopadhyay 2008, Gilhooley *et al*. 2007, Talha and Singh 2010, Mantari and Soares 2012, 2013, Neves *et al*. 2012a, b, Jha *et al*. 2013, Thai and Kim 2013, Thai and Choi 2013b, Zenkour 2013b). Some studies on response of FG sandwich plates have been carried out using higher-order shear deformation theories. Hamidi *et al*. (2012) and Abdelaziz *et al*. (2011) studied bending response, while Meiche *et al*. (2011) investigated vibration and buckling analysis of FG sandwich plates. Sobhy (2013) examined the vibration and buckling behavior of exponential FG sandwich plates resting on elastic foundations under various boundary conditions. By using quasi-3D higher-order shear deformation theories, which the stretching and shear deformation effects are taken into account, Neves *et al*. (2012c) and Zenkour (2013a) investigated bending analysis, while Bessaim *et al*. (2013) focused on both bending and free vibration of FG sandwich plates. A n-order shear deformation theory and a 3D linear theory of elasticity were proposed by Xiang *et al*. (2011) and Li *et al*. (2008) for free vibration of FG sandwich plates. Literature surveys reveal that although there are some research works reported on FG sandwich plates, the studies on bending, buckling and vibration responses of these structures in a unified fashion are a few in number. By using different shear deformation theories, Zenkour (2005a, b) investigated bending, vibration and buckling problem of sandwich plates with FG faces and homogeneous hardcore. These problems were also solved by Neves *et al*. (2013) by using a quasi-3D high-order shear deformation theory and a meshless technique. Thai *et al*. (2014) presented a new FSDT for sandwich plates composed of FG face sheets and an isotropic homogeneous core.

The objective of this study is to propose a higher-order shear deformation theory for bending, vibration and buckling analysis of FG sandwich plates in a unified fashion. The proposed theory contains only four unknowns, accounts for a hyperbolic distribution of transverse shear stress and satisfies the traction free boundary conditions. Equations of motion are derived from Hamilton's principle. The Navier-type and finite element solutions are derived for plate with simply-supported and various boundary conditions, respectively. Numerical results are obtained for FG sandwich plates with homogeneous hardcore and softcore to investigate the effects of the power-law index, thickness ratio of layers and side-to-thickness ratio on the deflections, stresses, critical buckling loads and natural frequencies.

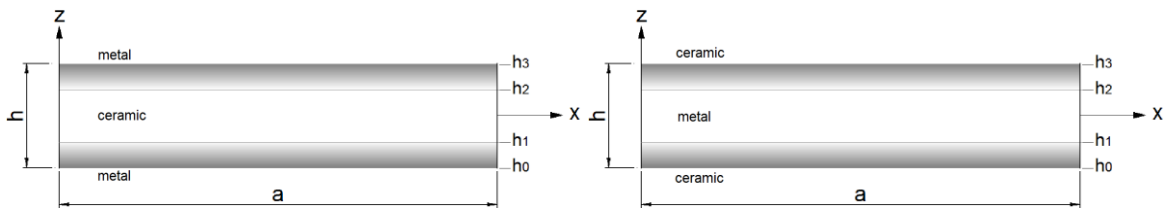

(a) Homogeneous hardcore (b) Homogeneous softcore

Fig. 1 Geometry of functionally graded sandwich plates

2. Problem formulation

Consider a three-layer sandwich plate as in Fig. 1. The face layers are made of a ceramic-metal material and the core layer is constituted by an isotropic material. The vertical positions of the bottom and top surfaces, and of two interfaces between the layers are denoted by $h_0 = -h/2$, h_1, h_2, $h_3 = h/2$, respectively. Here, h is the plate thickness, h_1, h_2 vary according the thickness ratio of layers.

2.1 Kinematics and strains

The displacement field of the present study is expressed by

$$\begin{aligned} u_1(x,y,z) &= u(x,y) - zw_{b,x} - \psi(z)w_{s,x} \\ u_2(x,y,z) &= v(x,y) - zw_{b,y} - \psi(z)w_{s,xy} \\ u_3(x,y,z) &= w_b(x,y) + w_s(x,y) \end{aligned} \tag{1}$$

where the comma indicates partial differentiation with respect to the coordinate subscript that follows, the shape function $\psi(z)$ at location z is given by (Grover *et al*. 2013)

$$\psi(z) = z\left(1 + \frac{6}{h\sqrt{13}}\right) - \sinh^{-1}\left(\frac{3z}{h}\right) \tag{2}$$

and u, v, w_b and w_s are the four unknown displacements of the mid-plane of the plate. The in-plane and out-of-plane strains associated with the displacement field in Eq. (1) are obtained

$$\begin{Bmatrix} \varepsilon_{xx} \\ \varepsilon_{yy} \\ \gamma_{xy} \end{Bmatrix} = \begin{Bmatrix} \varepsilon_{xx}^{(0)} \\ \varepsilon_{yy}^{(0)} \\ \gamma_{xy}^{(0)} \end{Bmatrix} + z\begin{Bmatrix} \varepsilon_{xx}^{(1)} \\ \varepsilon_{yy}^{(1)} \\ \gamma_{xy}^{(1)} \end{Bmatrix} + \psi\begin{Bmatrix} \varepsilon_{xx}^{(2)} \\ \varepsilon_{yy}^{(2)} \\ \gamma_{xy}^{(2)} \end{Bmatrix} \tag{3a}$$

$$\begin{Bmatrix} \gamma_{xz} \\ \gamma_{yz} \end{Bmatrix} = g\begin{Bmatrix} \gamma_{xz}^{(0)} \\ \gamma_{yz}^{(0)} \end{Bmatrix} \tag{3b}$$

where $g(z) = 1 - \psi_{,z}$; $\varepsilon^{(0)}$ are membrane strains; $\varepsilon^{(1)}$, $\varepsilon^{(2)}$ are curvatures and $\gamma^{(0)}$ are transverse shear strains. These strains are related to the displacements as follows

$$\begin{Bmatrix} \varepsilon_{xx}^{(0)} \\ \varepsilon_{yy}^{(0)} \\ \gamma_{xy}^{(0)} \end{Bmatrix} = \begin{Bmatrix} u_{,x} \\ v_{,y} \\ u_{,y} + v_{,x} \end{Bmatrix}, \begin{Bmatrix} \varepsilon_{xx}^{(1)} \\ \varepsilon_{yy}^{(1)} \\ \gamma_{xy}^{(1)} \end{Bmatrix} = \begin{Bmatrix} -w_{b,xx} \\ -w_{b,yy} \\ -2w_{b,xy} \end{Bmatrix}, \begin{Bmatrix} \varepsilon_{xx}^{(2)} \\ \varepsilon_{yy}^{(2)} \\ \gamma_{xy}^{(2)} \end{Bmatrix} = \begin{Bmatrix} -w_{s,xx} \\ -w_{s,yy} \\ -2w_{s,xy} \end{Bmatrix} \tag{4a}$$

$$\begin{Bmatrix} \gamma_{xz}^{(0)} \\ \gamma_{yz}^{(0)} \end{Bmatrix} = \begin{Bmatrix} w_{s,x} \\ w_{s,y} \end{Bmatrix} \tag{4b}$$

Eqs. (3a) and (3b) can be rewritten in a compact form as

$$\varepsilon = \varepsilon^{(0)} + z\varepsilon^{(1)} + \psi\varepsilon^{(2)} \tag{5a}$$

$$\gamma = g\gamma^{(0)} \tag{5b}$$

2.2 Equations of motion

Hamilton's principle is herein used to derive the equations of motion

$$0 = \int_0^T \left(\delta U + \delta V - \delta K\right) dt \tag{6}$$

where δU, δV, and δK are the variations of strain energy, work done, and kinetic energy, respectively.

The variation of strain energy is calculated by

$$\begin{aligned}\delta U &= \int_A \sum_{j=1}^{3} \int_{-h/2}^{h/2} \left(\sigma_{xx}^{(j)}\delta\varepsilon_{xx} + \sigma_{yy}^{(j)}\delta\varepsilon_{yy} + \sigma_{xy}^{(j)}\delta\gamma_{xy} + \sigma_{xz}^{(j)}\delta\gamma_{xz} + \sigma_{yz}^{(j)}\delta\gamma_{yz}\right) dA dz \\ &= \int_A \Big[N_{xx}\delta u_{,x} - M_{xx}^{b}\delta w_{b,xx} - M_{xx}^{s}\delta w_{s,xx} + N_{yy}\delta v_{,y} - M_{yy}^{b}\delta w_{b,yy} - M_{yy}^{s}\delta w_{s,yy} \\ &\quad + N_{xy}\left(\delta u_{,y} + \delta v_{,x}\right) - 2M_{xy}^{b}\delta w_{b,xy} - 2M_{xy}^{s}\delta w_{s,xy} + Q_x\delta w_{s,x} + Q_y\delta w_{s,y} \Big] dA\end{aligned} \tag{7}$$

where N, M, and Q are the stress resultants defined by

$$\left(N_{xx}, N_{yy}, N_{xy}\right) = \sum_{j=1}^{3} \int_{h_{j-1}}^{h_j} \left(\sigma_{xx}^{(j)}, \sigma_{yy}^{(j)}, \sigma_{xy}^{(j)}\right) dz \tag{8a}$$

$$\left(M_{xx}^{b}, M_{yy}^{b}, M_{xy}^{b}\right) = \sum_{j=1}^{3} \int_{h_{j-1}}^{h_j} z\left(\sigma_{xx}^{(j)}, \sigma_{yy}^{(j)}, \sigma_{xy}^{(j)}\right) dz \tag{8b}$$

$$\left(M_{xx}^{s}, M_{yy}^{s}, M_{xy}^{s}\right) = \sum_{j=1}^{3} \int_{h_{j-1}}^{h_j} \psi\left(\sigma_{xx}^{(j)}, \sigma_{yy}^{(j)}, \sigma_{xy}^{(j)}\right) dz \tag{8c}$$

$$\left(Q_x, Q_y\right) = \sum_{j=1}^{3} \int_{h_{j-1}}^{h_j} g\left(\sigma_{xz}^{(j)}, \sigma_{yz}^{(j)}\right) dz \tag{8d}$$

The variation of work done by in-plane loads $\bar{N}$ and transverse loads q is expressed by

$$\delta V = -\int_A \bar{N}\delta w dA - \int_A q\delta w dA \tag{9}$$

where $\bar{N} = N_{xx}^{0}(w_{b,xx} + w_{s,xx}) + 2N_{xy}^{0}(w_{b,xy} + w_{s,xy}) + N_{yy}^{0}(w_{b,yy} + w_{s,yy})$.

The variation of kinetic energy is determined by

$$\begin{aligned}\delta K &= \int_V (\dot{u}_1\delta\dot{u}_1 + \dot{u}_2\delta\dot{u}_2 + \dot{u}_3\delta\dot{u}_3)\rho(z)dAdz \\ &= \int_A I_0[\dot{u}\delta\dot{u} + \dot{v}\delta\dot{v} + (\dot{w}_b + \dot{w}_s)\delta(\dot{w}_b + \dot{w}_s)] - I_1(\dot{u}\delta\dot{w}_{b,x} + \dot{w}_{b,x}\delta\dot{u} + \dot{v}\delta\dot{w}_{b,y} + \dot{w}_{b,y}\delta\dot{v}) \\ &+ I_2(\dot{w}_{b,x}\delta\dot{w}_{b,x} + \dot{w}_{b,y}\delta\dot{w}_{b,y}) - J_1(\dot{u}\delta\dot{w}_{s,x} + \dot{w}_{s,x}\delta\dot{u} + \dot{v}\delta\dot{w}_{s,y} + \dot{w}_{s,y}\delta\dot{v}) \\ &+ K_2(\dot{w}_{s,x}\delta\dot{w}_{s,x} + \dot{w}_{s,y}\delta\dot{w}_{s,y}) + J_2(\dot{w}_{b,x}\delta\dot{w}_{s,x} + \dot{w}_{s,x}\delta\dot{w}_{b,x} + \dot{w}_{b,y}\delta\dot{w}_{s,y} + \dot{w}_{s,y}\delta\dot{w}_{b,y})dA\end{aligned} \tag{10}$$

where the dot-superscript convention indicates the differentiation with respect to the time variable t, $\rho(z)$ is the mass density, and the inertia terms I_i, J_i, K_i are expressed by

$$\left(I_0, I_1, I_2\right) = \sum_{j=1}^{3}\int_{h_{j-1}}^{h_j}\left(1, z, z^2\right)\rho\left(z\right)dz \tag{11a}$$

$$\left(J_1, J_2, K_2\right) = \sum_{j=1}^{3}\int_{h_{j-1}}^{h_j}\left(\psi, z\psi, \psi^2\right)\rho\left(z\right)dz \tag{11b}$$

Substituting Eqs. (7), (9), and (10) into Eq. (6), integrating by parts, and collecting the coefficients δu, δv, δw_b, δw_s, the following equations of motion are obtained

$$\delta u: \quad N_{xx,x} + N_{xy,y} = I_0\ddot{u} + I_1\ddot{w}_{b,x} - J_1\ddot{w}_{s,x} \tag{12a}$$

$$\delta v: \quad N_{xy,x} + N_{yy,y} = I_0\ddot{v} - I_1\ddot{w}_{b,y} - J_1\ddot{w}_{s,y} \tag{12b}$$

$$\begin{aligned}\delta w_b: \quad & M^b_{xx,xx} + 2M^b_{xy,xy} + M^b_{yy,yy} + \overline{N} + q \\ & = I_0(\ddot{w}_b + \ddot{w}_s) + I_1(\ddot{u}_x + \ddot{v}_y) - I_2(\ddot{w}_{b,xx} + \ddot{w}_{b,yy}) - J_2(\ddot{w}_{s,xx} + \ddot{w}_{s,yy})\end{aligned} \tag{12c}$$

$$\begin{aligned}\delta w_s: \quad & M^s_{xx,xx} + 2M^s_{xy,xy} + M^s_{yy,yy} + Q_{x,x} + Q_{y,y} + \overline{N} + q \\ & = I_0(\ddot{w}_b + \ddot{w}_s) + J_1(\ddot{u}_{,x} + \ddot{v}_{,y}) - J_2(\ddot{w}_{b,xx} + \ddot{w}_{b,yy}) - K_2(\ddot{w}_{s,xx} + \ddot{w}_{s,yy})\end{aligned} \tag{12d}$$

2.3 Constitutive equations

The effective material properties of FG sandwich plates according to the power-law form can be expressed by

$$P^{(j)}\left(z\right) = \left(P_b - P_t\right)V_b^{(j)} + P_t \tag{13}$$

where P_t and P_b are the Young's moduli (E), Poisson's ratio (ν), mass densities (ρ) of materials located at the top and bottom surfaces, and at the core, respectively. The volume fraction function $V_b^{(j)}$ defined by the power-law form as follows

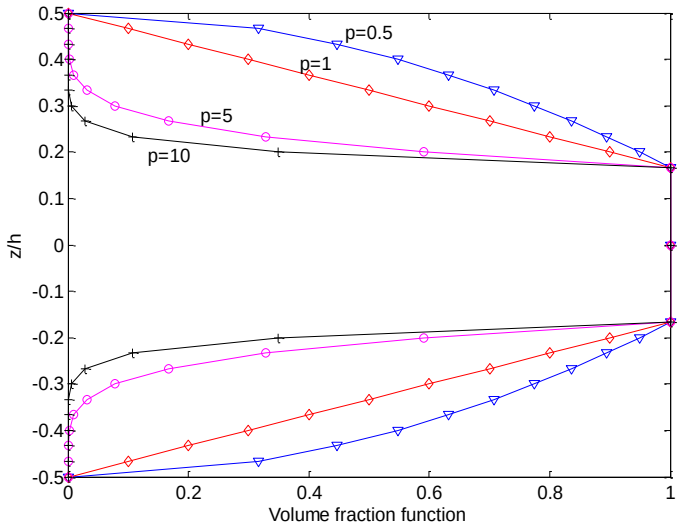

Fig. 2 Volume fraction function V_b with respect to the thickness ratio of layers (1-1-1)

$$\begin{cases} V_b^{(1)} = \left(\dfrac{z-h_0}{h_1-h_0} \right)^p & \text{for } z \in [h_0, h_1] \\ V_b^{(2)} = 1 & \text{for } z \in [h_1, h_2] \\ V_b^{(1)} = \left(\dfrac{z-h_3}{h_2-h_3} \right)^p & \text{for } z \in [h_2, h_3] \end{cases} \tag{14}$$

where p is a power-law index, which is positive. Distribution of material with V_b through the plate thickness for the thickness ratio of layers (1-1-1) is displayed in Fig. 2. The linear constitutive relations of the j-th layer of FG sandwich plates are written as

$$\begin{Bmatrix} \sigma_{xx}^{(j)} \\ \sigma_{yy}^{(j)} \\ \sigma_{xy}^{(j)} \end{Bmatrix} = \begin{bmatrix} C_{11}^{(j)} & C_{12}^{(j)} & 0 \\ C_{12}^{(j)} & C_{22}^{(j)} & 0 \\ 0 & 0 & C_{66}^{(j)} \end{bmatrix} \begin{Bmatrix} \varepsilon_{xx}^{(j)} \\ \varepsilon_{yy}^{(j)} \\ \gamma_{xy}^{(j)} \end{Bmatrix} \tag{15a}$$

$$\begin{Bmatrix} \sigma_{xz}^{(j)} \\ \sigma_{yz}^{(j)} \end{Bmatrix} = \begin{bmatrix} C_{55}^{(j)} & 0 \\ 0 & C_{44}^{(j)} \end{bmatrix} \begin{Bmatrix} \gamma_{xz} \\ \gamma_{yz} \end{Bmatrix} \tag{15b}$$

where

$$\begin{aligned} C_{11}^{(j)}(z) = C_{22}^{(j)}(z) = \frac{E^{(j)}(z)}{1-\nu^{(j)}(z)^2},\ C_{12}^{(j)}(z) = \nu^{(j)}(z) C_{11}^{(j)}(z) \\ C_{44}^{(j)}(z) = C_{55}^{(j)}(z) = C_{66}^{(j)}(z) = \frac{E^{(j)}(z)}{2\left[1+\nu^{(j)}(z)\right]} \end{aligned} \tag{16}$$

Substituting Eq. (3a) into Eq. (15a) and the subsequent results into Eqs. (8a), (8b) and (8c), the stress resultants are obtained in terms of strains as following compact form

$$\begin{Bmatrix} \mathbf{N} \\ \mathbf{M}^b \\ \mathbf{M}^s \end{Bmatrix} = \begin{bmatrix} \mathbf{A} & \mathbf{B} & \mathbf{B}^s \\ \mathbf{B} & \mathbf{D} & \mathbf{D}^s \\ \mathbf{B}^s & \mathbf{D}^s & \mathbf{H}^s \end{bmatrix} \begin{Bmatrix} \boldsymbol{\varepsilon}^{(0)} \\ \boldsymbol{\varepsilon}^{(1)} \\ \boldsymbol{\varepsilon}^{(2)} \end{Bmatrix} \tag{17}$$

where $\mathbf{A}$, $\mathbf{B}$, $\mathbf{D}$, $\mathbf{B}^s$, $\mathbf{D}^s$, $\mathbf{H}^s$ are the stiffnesses of the FG sandwich plate given by

$$\left(\mathbf{A},\mathbf{B},\mathbf{D},\mathbf{B}^s,\mathbf{D}^s,\mathbf{H}^s\right) = \sum_{j=1}^{3} \int_{h_{j-1}}^{h_j} \left(1, z, z^2, \psi, z\psi, \psi^2\right) \mathbf{C}^{(j)}(z)\, dz \tag{18}$$

where $\mathbf{C}^{(j)}(z)$ is reduced stiffness matrix of the j-th layer. Similarly, using Eqs. (3b), (15b) and (8d), the transverse shear forces can be calculated from the constitutive equations as

$$\begin{Bmatrix} Q_x \\ Q_y \end{Bmatrix} = \begin{bmatrix} A_{55}^s & 0 \\ 0 & A_{44}^s \end{bmatrix} \begin{Bmatrix} \gamma_{xz}^{(0)} \\ \gamma_{yz}^{(0)} \end{Bmatrix} \tag{19}$$

or in a compact form as

$$\mathbf{Q} = \mathbf{A}^s \boldsymbol{\gamma}^{(0)} \tag{20}$$

where the shear stiffnesses $\mathbf{A}^s$ of the FG sandwich plate are defined by

$$A_{44}^s = A_{55}^s = \sum_{j=1}^{3} \int_{h_{j-1}}^{h_j} g^2 C_{44}^{(j)}(z)\, dz = \sum_{j=1}^{3} \int_{h_{j-1}}^{h_j} g^2 C_{55}^{(j)}(z)\, dz \tag{21}$$

2.4 Equations of motion

Substituting Eqs. (17) and (20) into Eq. (12), the equations of motion can be expressed in terms of displacements (u, v, w_b, w_s) as follow

$$\begin{aligned} &A_{11}u_{,xx} + A_{66}u_{,yy} + \left(A_{12} + A_{66}\right)v_{,xy} - B_{11}w_{b,xxx} - \left(B_{12} + 2B_{66}\right)w_{b,xyy} - B_{11}^s w_{s,xxx} \\ &-\left(B_{12}^s + 2B_{66}^s\right)w_{s,xyy} = I_0\ddot{u} - I_1\ddot{w}_{b,x} - J_1\ddot{w}_{s,x} \end{aligned} \tag{22a}$$

$$\begin{aligned} &A_{22}v_{,yy} + A_{66}v_{,xx} + \left(A_{12} + A_{66}\right)u_{,xy} - B_{22}w_{b,yyy} - \left(B_{12} + 2B_{66}\right)w_{b,xxy} - B_{22}^s w_{s,yyy} \\ &-\left(B_{12}^s + 2B_{66}^s\right)w_{s,xxy} = I_0\ddot{v} - I_1\ddot{w}_{b,y} - J_1\ddot{w}_{s,y} \end{aligned} \tag{22b}$$

$$\begin{aligned} &B_{11}u_{,xxx} + \left(B_{12} + 2B_{66}\right)u_{,xyy} + \left(B_{12} + 2B_{66}\right)v_{,xxy} + B_{22}v_{,yyy} - D_{11}w_{b,xxxx} - D_{22}w_{b,yyyy} \\ &-2\left(D_{12} + 2D_{66}\right)w_{b,xxyy} - D_{11}^s w_{s,xxxx} - D_{22}^s w_{s,yyyy} - 2\left(D_{12}^s + 2D_{66}^s\right)w_{s,xxyy} + \bar{N} + q \\ &= I_0\left(\ddot{w}_b + \ddot{w}_s\right) + I_1\left(\ddot{u}_{,x} + \ddot{v}_{,y}\right) - I_2\left(\ddot{w}_{b,xx} + \ddot{w}_{b,yy}\right) - J_2\left(\ddot{w}_{s,xx} + \ddot{w}_{s,yy}\right) \end{aligned} \tag{22c}$$

$$\begin{aligned}
&B_{11}^s u_{,xxx} + \left(B_{11}^s + 2B_{66}^s\right)u_{,xyy} + \left(B_{12}^s + 2B_{66}^s\right)v_{,xxy} + B_{22}^s v_{,yyy} - D_{11}^s w_{b,xxxx} - D_{22}^s w_{b,yyyy} \\
&- 2\left(D_{12}^s + 2D_{66}^s\right)w_{b,xxyy} - H_{11}^s w_{s,xxxx} - H_{22}^s w_{s,yyyy} \\
&- 2\left(H_{12}^s + 2H_{66}^s\right)w_{s,xxyy} + A_{55}^s w_{s,xx} + A_{44}^s w_{s,yy} + \bar{N} + q \\
&= I_0\left(\ddot{w}_b + \ddot{w}_s\right) + J_1\left(\ddot{u}_{,x} + \ddot{v}_{,y}\right) - J_2\left(\ddot{w}_{b,xx} + \ddot{w}_{b,yy}\right) - K_2\left(\ddot{w}_{s,xx} + \ddot{w}_{s,yy}\right)
\end{aligned} \tag{22d}$$

2.5 Analytical solution for simply-supported FG sandwich plates

Consider a simply supported FG rectangular sandwich plate with length a and width b (Fig. 1). The Navier solution procedure is used to obtain the analytical solutions for the simply-supported boundary conditions, which are given by

$$\begin{aligned}
v = w_b = w_s = N_{xx} = M_{xx}^b = M_{xx}^s \quad &\text{on edges} \quad x = 0, a \\
u = w_b = w_s = N_{yy} = M_{yy}^b = M_{yy}^s \quad &\text{on edges} \quad x = 0, b
\end{aligned} \tag{23}$$

The solution is assumed to be of the form

$$u(x,y,t) = \sum_{m=1}^{\infty}\sum_{n=1}^{\infty} U_{mn} \cos\lambda x \sin\mu y \, e^{i\omega t} \tag{24a}$$

$$v(x,y,t) = \sum_{m=1}^{\infty}\sum_{n=1}^{\infty} V_{mn} \sin\lambda x \cos\mu y \, e^{i\omega t} \tag{24b}$$

$$w_b(x,y,t) = \sum_{m=1}^{\infty}\sum_{n=1}^{\infty} W_{bmn} \sin\lambda x \sin\mu y \, e^{i\omega t} \tag{24c}$$

$$w_s(x,y,t) = \sum_{m=1}^{\infty}\sum_{n=1}^{\infty} W_{smn} \sin\lambda x \sin\mu y \, e^{i\omega t} \tag{24d}$$

where $\lambda = m\pi / a$, $\mu = n\pi / b$, ω is the frequency of free vibration of the plate, $\sqrt{i} = -1$ the imaginary unit. The transverse load q is also expanded in the double-Fourier sine series as

$$q(x,y) = \sum_{m=1}^{\infty}\sum_{n=1}^{\infty} Q_{mn} \sin\lambda x \sin\mu y \tag{25}$$

where $Q_{mn} = q_0$ for sinusoidally distributed load and $Q_{mn} = 16q_0 / mn\pi^2$ (m, n = 1, 3, 5…) for uniformly distributed load. Assuming that the plate is subjected to in-plane compressive loads of form: $N_{xx}^0 = -N_0$, $N_{yy}^0 = -\gamma N_0$ (here γ is non-dimensional load parameter), $N_{xy}^0 = 0$. Substituting Eqs. (24) and (25) into Eq. (22), the following problem is obtained

$$\left(\begin{bmatrix} k_{11} & k_{12} & k_{13} & k_{14} \\ k_{12} & k_{22} & k_{23} & k_{24} \\ k_{13} & k_{23} & k_{33}+\alpha & k_{34}+\alpha \\ k_{14} & k_{24} & k_{34}+\alpha & k_{44}+\alpha \end{bmatrix} - \omega^2 \begin{bmatrix} m_{11} & 0 & m_{13} & m_{14} \\ 0 & m_{22} & m_{23} & m_{24} \\ m_{13} & m_{23} & m_{33} & m_{34} \\ m_{14} & m_{24} & m_{34} & m_{44} \end{bmatrix}\right) \begin{Bmatrix} U_{mn} \\ V_{mn} \\ W_{bmn} \\ W_{smn} \end{Bmatrix} = \begin{Bmatrix} 0 \\ 0 \\ Q_{mn} \\ Q_{mn} \end{Bmatrix} \tag{26}$$

where

$$
\begin{aligned}
&k_{11} = A_{11}\lambda^2 + A_{66}\mu^2, k_{12} = \left(A_{12} + A_{66}\right)\lambda\mu, k_{13} = -B_{11}\lambda^3 - \left(B_{12} + 2B_{66}\right)\lambda\mu^2 \\
&k_{14} = -B_{11}^s\lambda^3 - \left(B_{12}^s + 2B_{66}^s\right)\lambda\mu^2, k_{22} = A_{66}\lambda^2 + A_{22}\mu^2, k_{23} = -B_{22}\mu^3 - \left(B_{12} + 2B_{66}\right)\lambda^2\mu \\
&k_{24} = -B_{22}^s\mu^3 - \left(B_{12}^s + 2B_{66}^s\right)\lambda^2\mu, k_{33} = D_{11}\lambda^4 + 2\left(D_{12} + 2D_{66}\right)\lambda^2\mu^2 + D_{22}\mu^4 \\
&k_{34} = D_{11}^s\lambda^4 + 2\left(D_{12}^s + 2D_{66}^s\right)\lambda^2\mu^2 + D_{22}^s\mu^4 \\
&k_{44} = H_{11}^s\lambda^4 + 2\left(H_{12}^s + 2H_{66}^s\right)\lambda^2\mu^2 + H_{22}^s\mu^4 + A_{55}^s\lambda^2 + A_{44}^s\mu^2 \\
&m_{11} = m_{22} = I_0, m_{13} = -\lambda I_1, m_{14} = -\lambda J_1, m_{23} = -\mu I_1, m_{24} = -\mu J_1 \\
&m_{33} = I_0 + I_2\left(\lambda^2 + \mu^2\right), m_{34} = I_0 + J_2\left(\lambda^2 + \mu^2\right), m_{44} = I_0 + K_2\left(\lambda^2 + \mu^2\right) \\
&\alpha = -N_0\left(\lambda^2 + \gamma\mu^2\right)
\end{aligned}
\tag{27}
$$

Eq. (26) is a general form for bending, buckling and free vibration analysis of FG sandwich plates under in-plane and transverse loads. In order to solve bending problem, the in-plane compressive load N_0 and mass matrix **M** are set to zeros. The critical buckling loads (N_{cr}) can be obtained from the stability problem $|K_{ij}| = 0$ while the free vibration problem is achieved by omitting both in-plane and transverse loads.

2.6 Finite element formulation

Weak forms of Eqs. (12a)-(12d) on the element domain A_e can be obtained as follows

$$\int_{A_e}\left[N_{xx}\delta u_{,x} + N_{xy}\delta u_{,y} + \left(I_0\ddot{u} - I_1\ddot{w}_{b,x} - J_1\ddot{w}_{s,x}\right)\delta u\right]dxdy = 0 \tag{28a}$$

$$\int_{A_e}\left[N_{xy}\delta v_{,x} + N_{yy}\delta v_{,y} + \left(I_0\ddot{v} - I_1\ddot{w}_{b,y} - J_1\ddot{w}_{s,y}\right)\delta v\right]dxdy = 0 \tag{28b}$$

$$
\begin{aligned}
&\int_{A_e}\Big[-M_{xx}^b\delta w_{b,xx} - 2M_{xy}^b\delta w_{b,xy} - M_{yy}^b\delta w_{b,yy} - q\delta w_b \\
&+\left(N_{xx}^0 w_{b,x} + N_{xy}^0 w_{b,y}\right)\delta w_{b,x} + \left(N_{xy}^0 w_{b,x} + N_{yy}^0 w_{b,y}\right)\delta w_{b,y} \\
&+I_0\left(\ddot{w}_b + \ddot{w}_s\right)\delta w_b - \left(I_1\ddot{u} - I_2\ddot{w}_{b,x} - J_2\ddot{w}_{s,x}\right)\delta w_{b,x} - \left(I_1\ddot{v} - I_2\ddot{w}_{b,y} - J_2\ddot{w}_{s,x}\right)\delta w_{b,y}\Big]dxdy
\end{aligned}
\tag{28c}
$$

$$
\begin{aligned}
&\int_{A_e}\Big[-M_{xx}^s\delta w_{s,xx} - 2M_{xy}^s\delta w_{s,xy} - M_{yy}^s\delta w_{s,yy} + Q_x\delta w_{s,x} + Q_y\delta w_{s,y} - q\delta w_s \\
&+\left(N_{xx}^0 w_{s,x} + N_{xy}^0 w_{s,y}\right)\delta w_{s,x} + \left(N_{xy}^0 w_{s,x} + N_{yy}^0 w_{s,y}\right)\delta w_{s,y} \\
&+I_0\left(\ddot{w}_b + \ddot{w}_s\right)\delta w_s - \left(J_1\ddot{u} - J_2\ddot{w}_{b,x} - K_2\ddot{w}_{s,x}\right)\delta w_{s,x} - \left(J_1\ddot{v} - J_2\ddot{w}_{b,y} - K_2\ddot{w}_{s,x}\right)\delta w_{s,y}\Big]dxdy
\end{aligned}
\tag{28d}
$$

A $\mathbf{C}^1$ four-node quadrilateral element with ten degrees of freedom per node is used. The displacements on each element are expressed as a combination of Lagrangian linear interpolation functions ψ_j at the jth node for u and v and Hermitian cubic interpolation functions φ_j for w_b and w_s (see Thai and Choi 2013b)

$$u(x,y,t)=\sum_{j=1}^{m}\psi_j(x,y)u_j^e e^{i\omega t} \tag{29a}$$

$$v(x,y,t)=\sum_{j=1}^{m}\psi_j(x,y)v_j^e e^{i\omega t} \tag{29b}$$

$$w_b(x,y,t)=\sum_{j=1}^{m}\varphi_j(x,y)\Delta_{bj}^e e^{i\omega t} \tag{29c}$$

$$w_s(x,y,t)=\sum_{j=1}^{m}\varphi_j(x,y)\Delta_{sj}^e e^{i\omega t} \tag{29d}$$

where $(u_j^e,\ v_j^e)$ denote the values of $(u,\ v)$, $(\Delta_{bj}^e,\ \Delta_{sj}^e)$ denote the values of $(w_b,\ w_s)$ and their derivatives with respect to x and y, which are expressed by

$$\boldsymbol{\Delta}_b^e=\begin{bmatrix} w_b^e & w_{b,x}^e & w_{b,y}^e & w_{b,xy}^e \end{bmatrix}^T \tag{30a}$$

$$\boldsymbol{\Delta}_s^e=\begin{bmatrix} w_s^e & w_{s,x}^e & w_{s,y}^e & w_{s,xy}^e \end{bmatrix}^T \tag{30b}$$

and the interpolation functions ψ_j and φ_j for the jth node are given in terms of natural coordinates $(\xi,\ \eta)$ as

$$\psi_j=\frac{1}{4}(1+\xi_j\xi)(1-\eta_j\eta) \tag{31a}$$

$$\begin{aligned}
\varphi_{j1}&=\frac{1}{16}(\xi+\xi_j)^2(\xi\xi_j-2)(\eta+\eta_j)^2(\eta\eta_j-2)\\
\varphi_{j2}&=-\frac{1}{16}\xi_j(\xi+\xi_j)^2(1-\xi\xi_j)(\eta+\eta_j)^2(\eta\eta_j-2)\\
\varphi_{j3}&=-\frac{1}{16}(\xi+\xi_j)^2(\xi\xi_j-2)\eta_j(\eta+\eta_j)^2(\eta\eta_j-1)\\
\varphi_{j4}&=\frac{1}{16}\xi_j(\xi+\xi_j)^2(\xi\xi_j-1)\eta_j(\eta+\eta_j)^2(\eta\eta_j-1)
\end{aligned} \tag{31b}$$

Substituting Eqs. (29a)-(29d) into Eqs. (28a)-(28d) leads to

$$\left(\begin{bmatrix} \mathbf{K}^{11} & \mathbf{K}^{12} & \mathbf{K}^{13} & \mathbf{K}^{14} \\ {}^T\mathbf{K}^{12} & \mathbf{K}^{22} & \mathbf{K}^{23} & \mathbf{K}^{24} \\ {}^T\mathbf{K}^{13} & {}^T\mathbf{K}^{23} & \mathbf{K}^{33}+\mathbf{G} & \mathbf{K}^{34}+\mathbf{G} \\ {}^T\mathbf{K}^{14} & {}^T\mathbf{K}^{24} & {}^T\mathbf{K}^{34}+\mathbf{G} & \mathbf{K}^{44}+\mathbf{G} \end{bmatrix}-\omega^2\begin{bmatrix} \mathbf{M}^{11} & \mathbf{0} & \mathbf{M}^{13} & \mathbf{M}^{14} \\ \mathbf{0} & \mathbf{M}^{22} & \mathbf{M}^{23} & \mathbf{M}^{24} \\ {}^T\mathbf{M}^{13} & {}^T\mathbf{M}^{23} & \mathbf{M}^{33} & \mathbf{M}^{34} \\ {}^T\mathbf{M}^{14} & {}^T\mathbf{M}^{24} & {}^T\mathbf{M}^{34} & \mathbf{M}^{44} \end{bmatrix}\right)\begin{Bmatrix} \mathbf{u}^e \\ \mathbf{v}^e \\ \boldsymbol{\Delta}_b^e \\ \boldsymbol{\Delta}_s^e \end{Bmatrix}=\begin{Bmatrix} 0 \\ 0 \\ \mathbf{F}^3 \\ \mathbf{F}^4 \end{Bmatrix} \tag{32}$$

where the coefficients of the stiffness matrix **K**, **G**, mass matrix **M** and force vector **F** are defined as follows

$$K_{ij}^{11} = \int_{A_e} \left(A_{11}\psi_{i,x}\psi_{j,x} + A_{66}\psi_{i,y}\psi_{j,y} \right) dxdy \tag{33a}$$

$$K_{ij}^{12} = \int_{A_e} \left(A_{12}\psi_{i,x}\psi_{j,y} + A_{66}\psi_{i,y}\psi_{j,x} \right) dxdy \tag{33b}$$

$$K_{ij}^{13} = -\int_{A_e} \left[\psi_{i,x} \left(B_{11}\varphi_{j,xx} + B_{12}\varphi_{j,yy} \right) + 2\psi_{i,y} B_{66}\varphi_{j,xy} \right] dxdy \tag{33c}$$

$$K_{ij}^{14} = -\int_{A_e} \left[\psi_{i,x} \left(B_{11}^{s}\varphi_{j,xx} + B_{12}^{s}\varphi_{j,yy} \right) + 2\psi_{i,y} B_{66}^{s}\varphi_{j,xy} \right] dxdy \tag{33d}$$

$$K_{ij}^{22} = \int_{A_e} \left(A_{66}\psi_{i,x}\psi_{j,x} + A_{22}\psi_{i,y}\psi_{j,y} \right) dxdy \tag{33e}$$

$$K_{ij}^{23} = -\int_{A_e} \left[\psi_{i,y} \left(B_{22}\varphi_{j,yy} + B_{12}\varphi_{j,xx} \right) + 2\psi_{i,x} B_{66}\varphi_{j,xy} \right] dxdy \tag{33f}$$

$$K_{ij}^{24} = -\int_{A_e} \left[\psi_{i,y} \left(B_{22}^{s}\varphi_{j,yy} + B_{12}^{s}\varphi_{j,xx} \right) + 2\psi_{i,x} B_{66}^{s}\varphi_{j,xy} \right] dxdy \tag{33g}$$

$$K_{ij}^{33} = \int_{A_e} \left[D_{11}\varphi_{i,xx}\varphi_{j,xx} + D_{12} \left(\varphi_{i,xx}\varphi_{j,yy} + \varphi_{i,yy}\varphi_{j,xx} \right) + 4D_{66}\varphi_{i,xy}\varphi_{j,xy} + D_{22}\varphi_{i,yy}\varphi_{j,yy} \right] dxdy \tag{33h}$$

$$K_{ij}^{34} = \int_{A_e} \left[D_{11}^{s}\varphi_{i,xx}\varphi_{j,xx} + D_{12}^{s} \left(\varphi_{i,xx}\varphi_{j,yy} + \varphi_{i,yy}\varphi_{j,xx} \right) + 4D_{66}^{s}\varphi_{i,xy}\varphi_{j,xy} + D_{22}^{s}\varphi_{i,yy}\varphi_{j,yy} \right] dxdy \tag{33i}$$

$$\begin{aligned} K_{ij}^{44} = \int_{A_e} \Big[& H_{11}^{s}\varphi_{i,xx}\varphi_{j,xx} + H_{12}^{s} \left(\varphi_{i,xx}\varphi_{j,yy} + \varphi_{i,yy}\varphi_{j,xx} \right) + H_{22}^{s}\varphi_{i,yy}\varphi_{j,yy} + 4H_{66}^{s}\varphi_{i,xy}\varphi_{j,xy} \\ & + A_{55}^{s}\varphi_{i,x}\varphi_{j,x} + A_{44}^{s}\varphi_{i,y}\varphi_{j,y} \Big] dxdy \end{aligned} \tag{33j}$$

$$M_{ij}^{11} = M_{ij}^{22} = \int_{A_e} I_0\psi_i\psi_j dxdy \tag{33k}$$

$$M_{ij}^{13} = -\int_{A_e} I_1\psi_i\varphi_{j,x} dxdy \tag{33l}$$

$$M_{ij}^{14} = -\int_{A_e} J_1\psi_i\varphi_{j,x} dxdy \tag{33m}$$

$$M_{ij}^{23} = -\int_{A_e} I_1\psi_i\varphi_{j,y} dxdy \tag{33n}$$

$$M_{ij}^{24} = -\int_{A_e} J_1\psi_i\varphi_{j,y} dxdy \tag{33o}$$

$$M_{ij}^{33} = \int_{A_e} \left[I_0\varphi_i\varphi_j + I_2 \left(\varphi_{i,x}\varphi_{j,x} + \varphi_{i,y}\varphi_{j,y} \right) \right] dxdy \tag{33p}$$

$$M_{ij}^{34} = \int_{A_e} \left[I_0\varphi_i\varphi_j + J_2 \left(\varphi_{i,x}\varphi_{j,x} + \varphi_{i,y}\varphi_{j,y} \right) \right] dxdy \tag{33q}$$

$$M_{ij}^{44} = \int_{A_e} \left[I_0 \varphi_i \varphi_j + K_2 \left(\varphi_{i,x} \varphi_{j,x} + \varphi_{i,y} \varphi_{j,y} \right) \right] dxdy \tag{33r}$$

$$F_{ij}^3 = F_{ij}^4 = \int_{A_e} q \varphi_i dxdy \tag{33s}$$

$$G_{ij} = \int_{A_e} \left[N_{xx}^0 \varphi_{i,x} \varphi_{j,x} + N_{xy}^0 \left(\varphi_{i,x} \varphi_{j,y} + \varphi_{i,y} \varphi_{j,x} \right) + N_{yy}^0 \varphi_{i,y} \varphi_{j,y} \right] dxdy \tag{33t}$$

where the integrations in Eqs. (33) are numerically evaluated by Gauss quadrature integration rule.

3. Numerical results and discussion

In this section, a number of numerical examples are analyzed to verify the accuracy of present study and investigate the deflections, stresses, natural frequencies and critical buckling loads of FG sandwich plates. Two material combinations of metal and ceramic: Al/ZrO_2 and Al/Al_2O_3 are considered. Their material properties are given in Table 1. Four types of boundary conditions are considered: simply supported edges (SSSS), clamped edges (CCCC), clamped-simply supported edges (CSCS: clamped at $x = 0$, a and simply supported at $y = 0$, b) and clamped-free edges (CFCF: clamped at $x = 0$, a and free at $y = 0$, b). Due to the symmetry, only quarter-plate model is used in the finite element modeling to reduce computational cost. A convergence study is carried out and the mesh size of 4 × 4 is sufficient to obtain an accurate solution. Unless mentioned otherwise, two cases of SSSS FG sandwich plates are considered:

- Hardcore: homogeneous core with Al_2O_3 or ZrO_2 (E_b, ν_b, ρ_b) and FG faces with top and bottom surfaces made of Al (E_t, ν_t, ρ_t)
- Softcore: homogeneous core with Al (E_b, ν_b, ρ_b) and FG faces with top and bottom surfaces made of Al_2O_3 (E_t, ν_t, ρ_t)

For convenience, the following non-dimensional parameters are used

$$\begin{aligned}
&\bar{u}_3 = \frac{10E_0 h}{q_0 a^2} u_3\left(\frac{a}{2}, \frac{b}{2}\right),\ \hat{u}_3 = \frac{100E_m h^3}{12\left(1-\nu_m^2\right) q_0 a^4} u_3\left(\frac{a}{2}, \frac{b}{2}\right) \\
&\bar{\sigma}_{xx}(z) = \frac{10h^2}{q_0 a^2} \sigma_{xx}\left(\frac{a}{2}, \frac{b}{2}, z\right),\ \bar{\sigma}_{xz}(z) = \frac{h}{q_0 a} \sigma_{xz}\left(0, \frac{b}{2}, z\right) \\
&\bar{N} = \frac{N_{cr} a^2}{100E_0 h^3},\ \bar{\omega} = \omega \frac{a^2}{h} \sqrt{\rho_0 / E_0},\ E_0 = 1\text{GPa},\ \rho_0 = 1\text{kg/m}^3
\end{aligned} \tag{34}$$

Table 1 Material properties of metal and ceramic

Materials	Young's modulus (GPa)	Mass density (kg/m3)	Poisson's ratio
Aluminum (Al)	70	2707	0.3
Zirconia (ZrO_2)	151	3000	0. 3
Zirconia ($^*ZrO_2$)	200	5700	0. 3
Alumina (Al_2O_3)	380	3800	0.3

where E_m and ν_m are the Young's modulus and Poisson's ratio of metal, respectively.

3.1 Results for bending analysis

For verification purpose, the center deflections, axial and transverse shear stresses of Al/ZrO_2 sandwich plates under sinusoidal loads are calculated in Tables 2-4. The present results are compared with those predicted by different shear deformation theories (FSDT, TSDT, SSDT and quasi-3D). It can be seen that the obtained results agree well with those reported by Zenkour (2005a, 2013a), Neves *et al*. (2012c) and Bessaim *et al*. (2013), except some values of transverse shear stress. The present analytical solutions are better predictions with quasi-3D ones, which included both transverse shear and normal deformations, than TSDT and SSDT ones. The effects of the power-law index, thickness ratio of layers and side-to-thickness ratio on deflections, axial and shear stresses of Al/Al_2O_3 sandwich plates with homogeneous hardcore and softcore are given

Table 2 Nondimensional center deflections $\bar{u}_3$ of Al/ZrO_2 sandwich square plates with homogeneous hard-core (b/h = 10)

p	Theory	1-0-1	2-1-2	2-1-1	1-1-1	2-2-1	1-2-1
0	Present (analytical)	0.19581	0.19581	0.19581	0.19581	0.19581	0.19581
	Present (FEM)	0.19706	0.19706	0.19706	0.19706	0.19706	0.19706
	Zenkour (2005a) (FSDT)	0.19607	0.19607	-	0.19607	0.19607	0.19607
	Zenkour (2005a) (TSDT)	0.19606	0.19606	-	0.19606	0.19606	0.19606
	Zenkour (2005a) (SSDT)	0.19605	0.19605	-	0.19605	0.19605	0.19605
	Zenkour (2013a) (Quasi-3D)	0.19487	0.19487	-	0.19487	0.19487	0.19487
	Neves *et al*. (2012c) (Quasi-3D)	-	0.19490	0.19490	0.19490	0.19490	0.19490
	Bessaim *et al*. (2013) (Quasi-3D)	-	0.19486	0.19486	0.19486	0.19486	0.19486
1	Present	0.32300	0.30583	0.29637	0.29163	0.28054	0.27073
	Present (FEM)	0.32509	0.30782	0.29826	0.29352	0.28234	0.27248
	Zenkour (2005a) (FSDT)	0.32484	0.30750	-	0.29301	0.28168	0.27167
	Zenkour (2005a) (TSDT)	0.32358	0.30632		0.29199	0.28085	0.27094
	Zenkour (2005a) (SSDT)	0.32349	0.30624		0.29194	0.28082	0.27093
	Zenkour (2013a) (Quasi-3D)	0.32001	0.30275		0.28867	0.27760	0.26815
	Neves *et al*. (2012c) (Quasi-3D)	-	0.30700	0.29750	0.29290	0.28200	0.27220
	Bessaim *et al*. (2013) (Quasi-3D)	-	0.30430	0.29448	0.29007	0.27874	0.26915
2	Present	0.37245	0.35158	0.33726	0.33237	0.31575	0.30237
	Present (FEM)	0.37487	0.35387	0.33940	0.33453	0.31776	0.30434
	Zenkour (2005a) (FSDT)	0.37514	0.35408	-	0.33441	0.31738	0.30370
	Zenkour (2005a) (TSDT)	0.37335	0.35231	-	0.33289	0.31617	0.30263
	Zenkour (2005a) (SSDT)	0.37319	0.35218	-	0.33280	0.31611	0.30260
	Zenkour (2013a) (Quasi-3D)	0.36891	0.34737	-	0.32816	0.31152	0.29874
	Neves *et al*. (2012c) (Quasi-3D)	-	0.35190	0.33760	0.33290	0.31640	0.30320
	Bessaim *et al*. (2013) (Quasi-3D)	-	0.35001	0.33495	0.33068	0.31356	0.30060

Table 2 Continued

p	Theory	1-0-1	2-1-2	2-1-1	1-1-1	2-2-1	1-2-1
5	Present	0.40799	0.39068	0.37234	0.37064	0.34900	0.33443
	Present (FEM)	0.41064	0.39323	0.37469	0.37306	0.35121	0.33661
	Zenkour (2005a) (FSDT)	0.41120	0.39418	-	0.37356	0.35123	0.33631
	Zenkour (2005a) (TSDT)	0.40927	0.39183	-	0.37145	0.34960	0.33480
	Zenkour (2005a) (SSDT)	0.40905	0.39160	-	0.37128	0.34950	0.33474
	Zenkour (2013a) (Quasi-3D)	0.40532	0.38612	-	0.36546	0.34361	0.32966
	Neves *et al*. (2012c) (Quasi-3D)	-	0.39050	0.37220	0.37050	0.34900	0.33470
	Bessaim *et al*. (2013) (Quasi-3D)	-	0.38934	0.36981	0.36902	0.34649	0.33255
10	Present	0.41645	0.40270	0.38363	0.38452	0.36142	0.34777
	Present (FEM)	0.41913	0.40533	0.38605	0.38703	0.36370	0.35004
	Zenkour (2005a) (FSDT)	0.41919	0.40657	-	0.38787	0.36395	0.34996
	Zenkour (2005a) (TSDT)	0.41772	0.40407	-	0.38551	0.36215	0.34824
	Zenkour (2005a) (SSDT)	0.41750	0.40376	-	0.38490	0.34916	0.34119
	Zenkour (2013a) (Quasi-3D)	0.41448	0.39856	-	0.37924	0.35577	0.34259
	Neves *et al*. (2012c) (Quasi-3D)	-	0.40260	0.38350	0.38430	0.36120	0.34800
	Bessaim *et al*. (2013) (Quasi-3D)	-	0.40153	0.38111	0.38303	0.35885	0.34591

Table 3 Nondimensional axial stress $\bar{\sigma}_{xx}$ (h / 2) of Al/ZrO_2 sandwich square plates with homogeneous hardcore (b/h = 10)

p	Theory	1-0-1	2-1-2	2-1-1	1-1-1	2-2-1	1-2-1
0	Present	1.99816	1.99816	1.99816	1.99816	1.99816	1.99816
	Present (FEM)	2.1514	2.1514	2.1514	2.1514	2.1514	2.1514
	Zenkour (2005a) (FSDT)	1.97576	1.97576	-	1.97576	1.97576	1.97576
	Zenkour (2005a) (TSDT)	2.04985	2.04985	-	2.04985	2.04985	2.04985
	Zenkour (2005a) (SSDT)	2.05452	2.05452	-	2.05452	2.05452	2.05452
	Zenkour (2013a) (Quasi-3D)	2.00773	2.00773	-	2.00773	2.00773	2.00773
	Neves *et al*. (2012c) (Quasi-3D)	-	2.00660	2.00640	2.00660	2.00650	2.00640
	Bessaim *et al*. (2013) (Quasi-3D)	-	1.99524	1.99524	1.99524	1.99524	1.99524
1	Present	1.54644	1.46498	1.35921	1.39614	1.29063	1.29390
	Present (FEM)	1.6334	1.5461	1.4418	1.4749	1.3699	1.3705
	Zenkour (2005a) (FSDT)	1.53245	1.45167	-	1.38303	1.27749	1.28096
	Zenkour (2005a) (TSDT)	1.57923	1.49587	-	1.42617	1.32062	1.32309
	Zenkour (2005a) (SSDT)	1.58204	1.49859	-	1.42892	1.32342	1.32590
	Zenkour (2013a) (Quasi-3D)	1.57004	1.48833	-	1.41781	1.30907	1.31204
	Neves *et al*. (2012c) (Quasi-3D)	-	1.48130	1.37680	1.41370	1.30920	1.31330
	Bessaim *et al*. (2013) (Quasi-3D)	-	1.46131	1.35053	1.39243	1.28274	1.29030

Table 3 Continued

p	Theory	1-0-1	2-1-2	2-1-1	1-1-1	2-2-1	1-2-1
2	Present	1.78579	1.68875	1.53218	1.59602	1.43915	1.44937
	Present (FEM)	1.8818	1.7745	1.6200	1.6778	1.5217	1.5280
	Zenkour (2005a) (FSDT)	1.77085	1.67496	-	1.58242	1.42528	1.43580
	Zenkour (2005a) (TSDT)	1.82167	1.72144	-	1.62748	1.47095	1.47988
	Zenkour (2005a) (SSDT)	1.82450	1.72412	-	1.63025	1.47387	1.48283
	Zenkour (2013a) (Quasi-3D)	1.81509	1.72030	-	1.62591	1.46372	1.47421
	Neves *et al*. (2012c) (Quasi-3D)	-	1.69940	1.54560	1.60880	1.45430	1.46590
	Bessaim *et al*. (2013) (Quasi-3D)	-	1.68472	1.52101	1.59170	1.42887	1.44497
5	Present	1.95216	1.87869	1.68134	1.78347	1.57842	1.60691
	Present (FEM)	2.0641	1.9704	1.7762	1.8686	1.6646	1.6875
	Zenkour (2005a) (FSDT)	1.93576	1.86479	-	1.76988	1.56401	1.59309
	Zenkour (2005a) (TSDT)	1.99272	1.91302	-	1.81580	1.61181	1.63814
	Zenkour (2005a) (SSDT)	1.99567	1.91547	-	1.81838	1.61477	1.64106
	Zenkour (2013a) (Quasi-3D)	1.97912	1.91504	-	1.82018	1.60953	1.63906
	Neves *et al*. (2012c) (Quasi-3D)	-	1.88380	1.69090	1.79060	1.58930	1.61950
	Bessaim *et al*. (2013) (Quasi-3D)	-	1.87516	1.66856	1.77919	1.56627	1.60203
10	Present	1.98591	1.93573	1.73141	1.85102	1.63059	1.67244
	Present (FEM)	2.1111	2.0316	1.8309	1.9381	1.7189	1.7539
	Zenkour (2005a) (FSDT)	1.96780	1.92165	-	1.83754	1.61645	1.65844
	Zenkour (2005a) (TSDT)	2.03036	1.97126	-	1.88376	1.66660	1.70417
	Zenkour (2005a) (SSDT)	2.03360	1.97313	-	1.88147	1.61979	1.64851
	Zenkour (2013a) (Quasi-3D)	2.00692	1.97075	-	1.89162	2.18558	1.67350
	Neves *et al*. (2012c) (Quasi-3D)	-	1.93970	1.74050	1.85590	1.63950	1.68320
	Bessaim *et al*. (2013) (Quasi-3D)	-	1.93266	1.71835	1.84705	1.61792	1.66754

Table 4 Nondimensional transverse shear stress $\bar{\sigma}_{xz}(0)$ of Al/ZrO_2 sandwich square plates with homogeneous hardcore (b/h = 10)

p	Theory	1-0-1	2-1-2	2-1-1	1-1-1	2-2-1	1-2-1
0	Present	0.27209	0.27209	0.27209	0.27209	0.27209	0.27209
	Present (FEM)	0.2702	0.2702	0.2702	0.2702	0.2702	0.2702
	Zenkour (2005a) (FSDT)	0.19099	0.19099	-	0.19099	0.19099	0.19099
	Zenkour (2005a) (TSDT)	0.23857	0.23857	-	0.23857	0.23857	0.23857
	Zenkour (2005a) (SSDT)	0.24618	0.24618	-	0.24618	0.24618	0.24618
	Zenkour (2013a) (Quasi-3D)	0.23910	0.23910	-	0.23910	0.23910	0.23910
	Neves *et al*. (2012c) (Quasi-3D)	-	0.25380	0.22910	0.24610	0.24110	0.23630
	Bessaim *et al*. (2013) (Quasi-3D)	-	0.23794	0.23794	0.23794	0.23794	0.23794

Table 4 Continued

p	Theory	1-0-1	2-1-2	2-1-1	1-1-1	2-2-1	1-2-1
1	Present	0.32334	0.30125	0.30369	0.29273	0.29237	0.28656
	Present (FEM)	0.3211	0.29916	0.30158	0.29070	0.29034	0.28457
	Zenkour (2005a) (FSDT)	0.26099	0.24316	-	0.23257	0.22762	0.22057
	Zenkour (2005a) (TSDT)	0.29203	0.27104	-	0.26117	0.25951	0.25258
	Zenkour (2005a) (SSDT)	0.29907	0.27774	-	0.26809	0.26680	0.26004
	Zenkour (2013a) (Quasi-3D)	0.36531	0.34366	-	0.32853	0.31785	0.30845
	Neves *et al*. (2012c) (Quasi-3D)	-	0.27450	0.26400	0.26430	0.25940	0.24960
	Bessaim *et al*. (2013) (Quasi-3D)	-	0.27050	0.27017	0.26060	0.25890	0.25196
2	Present	0.35524	0.31480	0.31961	0.30063	0.30066	0.29132
	Present (FEM)	0.35278	0.31262	0.31738	0.29855	0.29858	0.28930
	Zenkour (2005a) (FSDT)	0.29731	0.26752	-	0.25077	0.24316	0.23257
	Zenkour (2005a) (TSDT)	0.32622	0.28838	-	0.27188	0.26939	0.25834
	Zenkour (2005a) (SSDT)	0.33285	0.29422	-	0.27807	0.27627	0.26543
	Zenkour (2013a) (Quasi-3D)	0.41778	0.38601	-	0.36417	0.34824	0.33543
	Neves *et al*. (2012c) (Quasi-3D)	-	0.27600	0.28770	0.26680	0.26360	0.25230
	Bessaim *et al*. (2013) (Quasi-3D)	-	0.28792	0.28742	0.27138	0.26885	0.25776
5	Present	0.41674	0.33526	0.34435	0.31020	0.31131	0.29569
	Present (FEM)	0.41386	0.33293	0.34195	0.30805	0.30914	0.29364
	Zenkour (2005a) (FSDT)	0.34538	0.29731	-	0.27206	0.26099	0.24596
	Zenkour (2005a) (TSDT)	0.38634	0.31454	-	0.28643	0.28265	0.26512
	Zenkour (2005a) (SSDT)	0.39370	0.31930	-	0.29150	0.28895	0.27153
	Zenkour (2013a) (Quasi-3D)	0.46890	0.42723	-	0.39918	0.37791	0.36234
	Neves *et al*. (2012c) (Quasi-3D)	-	0.27120	0.33770	0.26550	0.26690	0.25460
	Bessaim *et al*. (2013) (Quasi-3D)	-	0.31419	0.31293	0.28606	0.28217	0.26463
10	Present	0.47099	0.35092	0.36250	0.31657	0.31837	0.29777
	Present (FEM)	0.46770	0.34846	0.35995	0.31436	0.31614	0.2957
	Zenkour (2005a) (FSDT)	0.37277	0.31316	-	0.28299	0.26998	0.25257
	Zenkour (2005a) (TSDT)	0.43206	0.33242	-	0.29566	0.29080	0.26895
	Zenkour (2005a) (SSDT)	0.44147	0.33644	-	0.29529	0.29671	0.27676
	Zenkour (2013a) (Quasi-3D)	0.49051	0.44435	-	0.41385	0.39045	0.37390
	Neves *et al*. (2012c) (Quasi-3D)	-	0.26710	0.38060	0.26390	0.26920	0.25680
	Bessaim *et al*. (2013) (Quasi-3D)	-	0.33210	0.32959	0.29534	0.29036	0.26850

in Tables 5-7. It can be seen that with the increase of power-law index, the deflections increase for sandwich plates with homogeneous hardcore, and decrease for ones with homogeneous softcore (Fig. 3). The variations of axial and shear stresses through the thickness of (1-2-1) sandwich plate with homogeneous hardcore are plotted in Fig. 4. The maximum axial stress is located inside the

plate for $p > 0$. For example, with $p = 10$ maximum axial stress is located at the interfaces of faces and core. Meanwhile, the maximum shear stress is located in the mid-plane of the plate (Fig. 4(b)).

Table 5 Nondimensional center deflections $\bar{u}_3$ of Al/Al_2O_3 sandwich square plates with homogeneous hardcore and softcore

Core	*b*/*h*	*p*	1-0-1	2-1-2	2-1-1	1-1-1	2-2-1	1-2-1
Hardcore	5	0	0.02248	0.02248	0.02248	0.02248	0.02248	0.02248
		0.5	0.03816	0.03543	0.03434	0.03346	0.03217	0.03084
		1	0.05327	0.04720	0.04476	0.04286	0.04009	0.03730
		5	0.10161	0.08770	0.07916	0.07489	0.06573	0.05748
		10	0.10996	0.09685	0.08701	0.08346	0.07255	0.06321
	10	0	0.07781	0.07781	0.07781	0.07781	0.07781	0.07781
		0.5	0.13759	0.12758	0.12319	0.12009	0.11500	0.10993
		1	0.19579	0.17329	0.16343	0.15660	0.14569	0.13494
		5	0.37990	0.33228	0.29728	0.28268	0.24614	0.21394
		10	0.40569	0.36793	0.32717	0.31662	0.27294	0.23663
Softcore	5	0	0.12201	0.12201	0.12201	0.12201	0.12201	0.12201
		0.5	0.04165	0.04658	0.04823	0.05035	0.05315	0.05587
		1	0.03285	0.03762	0.03885	0.04145	0.04384	0.04686
		5	0.02437	0.02797	0.02868	0.03163	0.03331	0.03732
		10	0.02337	0.02653	0.02720	0.03002	0.03158	0.03580
	10	0	0.42238	0.42238	0.42238	0.42238	0.42238	0.42238
		0.5	0.12984	0.14143	0.14975	0.15187	0.16356	0.17012
		1	0.10240	0.11192	0.11900	0.12083	0.13119	0.13655
		5	0.08054	0.08577	0.09074	0.09198	0.09976	0.10404
		10	0.07887	0.08302	0.08752	0.08852	0.09575	0.09985

Table 6 Nondimensional axial stress $\bar{\sigma}_{xx}(h/2)$ of Al/Al_2O_3 sandwich square plates with homogeneous hardcore and softcore

Core	*b*/*h*	*p*	1-0-1	2-1-2	2-1-1	1-1-1	2-2-1	1-2-1
Hardcore	5	0	2.06499	2.06499	2.06499	2.06499	2.06499	2.06499
		0.5	0.67811	0.62884	0.57977	0.59191	0.54395	0.54163
		1	0.96663	0.85597	0.75027	0.77382	0.67469	0.66676
		5	1.87021	1.63974	1.29282	1.39738	1.08565	1.05967
		10	1.99309	1.81363	1.41179	1.56386	1.19180	1.17174
	10	0	1.99816	1.99816	1.99816	1.99816	1.99816	1.99816
		0.5	0.66015	0.61190	0.56273	0.57540	0.52770	0.52564

Table 6 Continued

Core	*b*/*h*	*p*	1-0-1	2-1-2	2-1-1	1-1-1	2-2-1	1-2-1
Hardcore	10	1	0.94491	0.83618	0.73015	0.75472	0.65599	0.64846
		5	1.84076	1.61688	1.26621	1.37470	1.06237	1.03699
		10	1.95752	1.79109	1.38334	1.54156	1.16787	1.14867
Softcore	5	0	2.06499	2.06499	2.06499	2.06499	2.06499	2.06499
		0.5	3.37291	3.64881	4.19439	3.90261	4.58333	4.36193
		1	2.66925	2.88726	3.34333	3.09373	3.68874	3.47176
		5	2.12775	2.24453	2.54168	2.38099	2.80713	2.64695
		10	2.08876	2.18124	2.44351	2.30207	2.69319	2.54919
	10	0	1.99816	1.99816	1.99816	1.99816	1.99816	1.99816
		0.5	3.20390	3.45074	4.02743	3.69235	4.39708	4.14831
		1	2.52909	2.71004	3.20399	2.89735	3.52620	3.26777
		5	2.03584	2.10819	2.44190	2.20993	2.67847	2.44621
		10	2.00839	2.05744	2.35233	2.14077	2.57315	2.35050

Table 7 Nondimensional transverse shear stress $\bar{\sigma}_{xz}(0)$ of Al/Al_2O_3 sandwich square plates with homogeneous hardcore and softcore

Core	*b*/*h*	*p*	1-0-1	2-1-2	2-1-1	1-1-1	2-2-1	1-2-1
Hardcore	5	0	0.27096	0.27096	0.27096	0.27096	0.27096	0.27096
		0.5	0.32178	0.30204	0.30354	0.29395	0.29299	0.28747
		1	0.36388	0.32400	0.32711	0.30908	0.30742	0.29773
		5	0.58073	0.39103	0.40705	0.34678	0.34575	0.32084
		10	0.76034	0.42000	0.44374	0.35760	0.35821	0.32576
	10	0	0.27209	0.27209	0.27209	0.27209	0.27209	0.27209
		0.5	0.32265	0.30287	0.30441	0.29479	0.29385	0.28834
		1	0.36473	0.32475	0.32790	0.30983	0.30818	0.29848
		5	0.58197	0.39178	0.40786	0.34747	0.34642	0.32148
		10	0.76213	0.42075	0.44461	0.35830	0.35889	0.32641
Softcore	5	0	0.27096	0.27096	0.27096	0.27096	0.27096	0.27096
		0.5	0.15838	0.19508	0.18888	0.21699	0.21588	0.23615
		1	0.12365	0.16621	0.15851	0.19594	0.19422	0.22528
		5	0.07031	0.10933	0.10218	0.14659	0.14442	0.19659
		10	0.06038	0.09617	0.09006	0.13304	0.13106	0.18704
	10	0	0.27209	0.27209	0.27209	0.27209	0.27209	0.27209
		0.5	0.15951	0.19657	0.19019	0.21861	0.21742	0.23779
		1	0.12450	0.16751	0.15959	0.19749	0.19565	0.22694
		5	0.07070	0.11015	0.10278	0.14781	0.14545	0.19819
		10	0.06068	0.09685	0.09054	0.13414	0.13197	0.18860

To further verify the accuracy of the present theory, Table 8 shows the comparison of the deflections of a thick Al/*ZrO_2 CCCC square plate under uniform loads (b/h = 5). It can be seen that the obtained finite element solutions are close to those generated by Gilhooley *et al*. (2007) using a quasi-3D theory, and those of Nguyen-Xuan *et al*. (2012) and Lee *et al*. (2009) using the FSDT. The effects of the boundary conditions, the power-law index and thickness ratio of layers on deflections, axial and shear stresses of Al/ZrO_2 sandwich plates with homogeneous hardcore are given in Tables 9-11 and the variation of nondimensional axial and transverse shear stresses through the thickness of (2-2-1) Al/ZrO_2 CCCC sandwich plates is plotted in Fig. 5. It is seen that the deflections increase with an increase of the power-law index, lowest and highest ones correspond to the CCCC and CFCF cases, respectively.

Table 8 Nondimensional center deflections $\hat{u}_3$ of Al/*ZrO_2 CCCC square plates under uniform load (b/h = 5)

Theory	*p*			
	0	0.5	1	2
Present (FEM)	0.0745	0.0992	0.1156	0.1354
Gilhooley *et al*. (2007) (Quasi-3D)	0.0731	0.1073	0.1253	0.1444
Nguyen-Xuan *et al*. (2012) (FSDT)	0.0788	0.1051	0.1227	0.1420
Lee *et al*. (2009) (FSDT)	0.0774	0.1034	0.1207	0.1404

Table 9 Nondimensional center deflections $\bar{u}_3$ of Al/ZrO_2 sandwich square plates with homogeneous hardcore and various boundary conditions (b/h = 10)

Boundary conditions	*p*	1-0-1	2-1-2	2-1-1	1-1-1	2-2-1	1-2-1
CCCC	0	0.1128	0.1128	0.1128	0.1128	0.1128	0.1128
	0.5	0.1557	0.1495	0.1467	0.1448	0.1414	0.1381
	1	0.1824	0.1726	0.1675	0.1648	0.1588	0.1535
	5	0.2304	0.2187	0.2091	0.2073	0.1957	0.1878
	10	0.2365	0.2255	0.2156	0.2149	0.2024	0.1949
CSCS	0	0.1601	0.1601	0.1601	0.1601	0.1601	0.1601
	0.5	0.2225	0.2137	0.2095	0.2069	0.2018	0.1970
	1	0.2614	0.2474	0.2399	0.2361	0.2273	0.2195
	5	0.3302	0.3147	0.3003	0.2985	0.2813	0.2698
	10	0.3308	0.3245	0.3096	0.3095	0.2911	0.2803
CFCF	0	0.2238	0.2238	0.2238	0.2238	0.2238	0.2238
	0.5	0.3099	0.2977	0.2919	0.2882	0.2812	0.2747
	1	0.3636	0.3441	0.3338	0.3285	0.3163	0.3057
	5	0.4593	0.4369	0.4172	0.4143	0.3906	0.3748
	10	0.4709	0.4505	0.4302	0.4295	0.4042	0.3893

Table 10 Nondimensional axial stress $\bar{\sigma}_{xx}(h/2)$ of Al/ZrO_2 sandwich square plates with homogeneous hardcore and various boundary conditions (b/h = 10)

Boundary conditions	p	1-0-1	2-1-2	2-1-1	1-1-1	2-2-1	1-2-1
CCCC	0	1.6045	1.6045	1.6045	1.6045	1.6045	1.6045
	0.5	1.0350	0.9942	0.9513	0.9626	0.9189	0.9176
	1	1.2142	1.1489	1.0749	1.0966	1.0216	1.0206
	5	1.5345	1.4588	1.3215	1.3828	1.2374	1.2507
	10	1.5739	1.5044	1.3630	1.4335	1.2774	1.2988
CSCS	0	2.2066	2.2066	2.2066	2.2066	2.2066	2.2066
	0.5	1.4239	1.3677	1.3069	1.3236	1.2618	1.2603
	1	1.6747	1.5852	1.4801	1.5121	1.4062	1.4052
	5	2.1162	2.0199	1.8244	1.9155	1.7096	1.7300
	10	2.1646	2.0826	1.8807	1.9867	1.7655	1.7980
CFCF	0	2.7960	2.7960	2.7960	2.7960	2.7960	2.7960
	0.5	1.7988	1.7278	1.6531	1.6725	1.5963	1.5933
	1	2.1121	1.9999	1.8709	1.9082	1.7776	1.7745
	5	2.6704	2.5443	2.3050	2.4123	2.1588	2.1801
	10	2.7349	2.6235	2.3769	2.5015	2.2293	2.2650

Table 11 Nondimensional transverse shear stress $\bar{\sigma}_{xz}(0)$ of Al/ZrO_2 sandwich square plates with homogeneous hardcore and various boundary conditions (b/h = 10)

Boundary conditions	p	1-0-1	2-1-2	2-1-1	1-1-1	2-2-1	1-2-1
CCCC	0	0.4235	0.4235	0.4235	0.4235	0.4235	0.4235
	0.5	0.4734	0.4550	0.4568	0.4473	0.4466	0.4411
	1	0.5079	0.4733	0.4776	0.4598	0.4594	0.4498
	5	0.6544	0.5279	0.5452	0.4882	0.4923	0.4649
	10	0.7381	0.5528	0.5741	0.4984	0.5044	0.4682
CSCS	0	0.4319	0.4319	0.4319	0.4319	0.4319	0.4319
	0.5	0.4825	0.4638	0.4657	0.4559	0.4553	0.4497
	1	0.5176	0.4824	0.4870	0.4686	0.4683	0.4584
	5	0.6670	0.5380	0.5569	0.4974	0.5028	0.4738
	10	0.7523	0.5633	0.5867	0.5079	0.5151	0.4771
CFCF	0	0.6424	0.6424	0.6424	0.6424	0.6424	0.6424
	0.5	0.7181	0.6902	0.6930	0.6784	0.6775	0.6691
	1	0.7704	0.7180	0.7247	0.6974	0.6969	0.6823
	5	0.9926	0.8008	0.8282	0.7404	0.7475	0.7052
	10	1.1195	0.8385	0.8723	0.7560	0.7661	0.7101

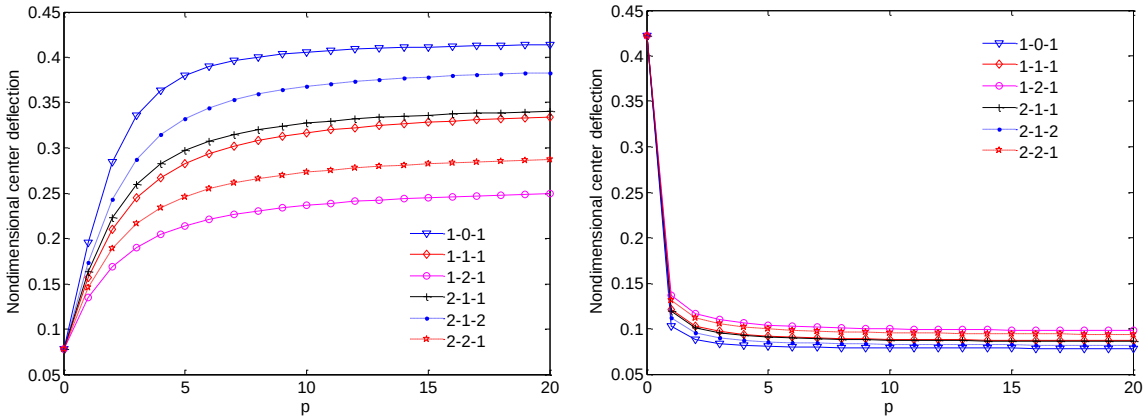

(a) Homogeneous hardcore (b) Homogeneous softcore

Fig. 3 Effect of the power-law index p on the nondimensional center deflections ($\bar{u}_3$) of Al/Al_2O_3 sandwich square plates (b/h = 10)

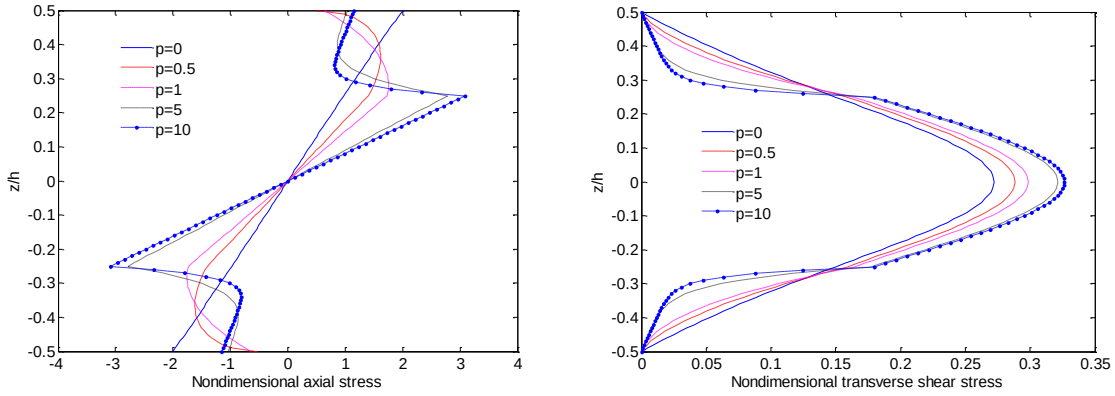

(a) Nondimensional axial stress $\bar{\sigma}_{xx}$ (b) Nondimensional shear stress $\bar{\sigma}_{xz}$

Fig. 4 Variation of the nondimensional axial and shear stresses through the thickness of (1-2-1) Al/Al_2O_3 sandwich square plates with homogeneous hardcore (b/h = 10)

3.2 Results for vibration and buckling analysis

To verify the accuracy of the present theory in predicting the vibration and buckling behavior of Al/Al_2O_3 sandwich plates, their fundamental frequencies and critical buckling loads are calculated. Tables 12-15 contain the fundamental frequencies and critical buckling loads for six types of SSSS sandwich plates with different values of the power-law index. For buckling analysis, two types of in-plane loads: uniaxial compression (γ = 0) and biaxial compressions (γ = 0.5, γ = 1) are considered. It should be noted that the solutions reported by Li *et al.* (2008) were based on 3D linear theory of elasticity, whereas Zenkour (2005b), Meiche *et al.* (2011) and Bessaim *et al.* (2013) were based on a TSDT, SSDT and HSDT as well as quasi-3D. It is clear that the results of present study again agree well with previous solutions (Meiche *et al.* 2011, Li *et al.* 2008, Zenkour

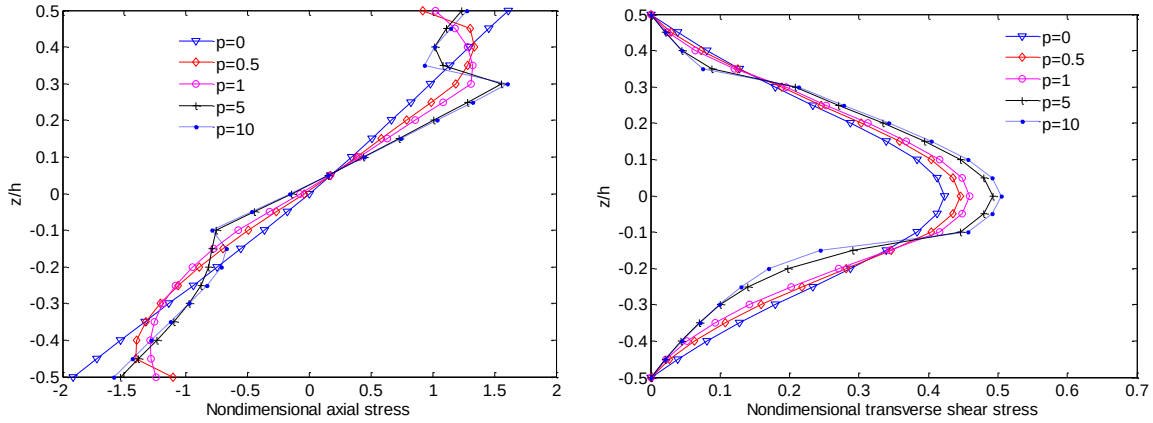

(a) Nondimensional axial stress $\bar{\sigma}_{xx}$ (b) Nondimensional shear stress $\bar{\sigma}_{xz}$

Fig. 5 Variation of the nondimensional axial and shear stresses through the thickness of (2-2-1) Al/ZrO_2 CCCC sandwich square plates with homogeneous hardcore (b/h = 10)

2005b). Besides, it is found that for vibration, the present solutions are more in close agreement with those of Bessaim *et al*. (2013) and Li *et al*. (2008) than with those of Meiche *et al*. (2011) and Zenkour (2005b) in many cases. It implies that the proposed theory predicts more accurate than TSDT, SSDT and HSDT's model. Figs. 6 and 7 show the fundamental frequencies and critical buckling loads of sandwich plates with respect to the power-law index. It can be seen from these figures that with the increase of the power-law index, they decrease for sandwich plates with homogeneous hardcore, and increase for ones with homogeneous softcore. Moreover, the effects of the boundary conditions on the fundamental frequency and critical buckling loads are also given in Tables 16 and 17. It is noticeable from Tables 5 and 12-17 and Figs. 3, 6 and 7 that, for homogeneous hardcore, the lowest and highest values of deflection correspond to the (1-2-1) and (1-0-1) sandwich plates, and conversely for results of buckling load and natural frequency, respectively. It is due to the fact that these plates correspond to the highest and lowest volume fractions of the ceramic phase, and thus makes them become the hardest and softest ones.

Table 12 Nondimensional fundamental frequency $\bar{\omega}$ of Al/Al_2O_3 sandwich square plates with homogeneous hardcore (b/h = 10)

p	Theory	1-0-1	2-1-2	2-1-1	1-1-1	2-2-1	1-2-1
0	Present	1.82562	1.82562	1.82562	1.82562	1.82562	1.82562
	Present (FEM)	1.8219	1.8219	1.8219	1.8219	1.8219	1.8219
	Zenkour (2005b) (TSDT)	1.82445	1.82445	1.82445	1.82445	1.82445	1.82445
	Zenkour (2005b) (SSDT)	1.82452	1.82452	1.82452	1.82452	1.82452	1.82452
	Meiche *et al*. (2011) (HSDT)	1.82449	1.82449	1.82449	1.82449	1.82449	1.82449
	Bessaim *et al*. (2013) (Quasi-3D)	1.82682	1.82682	-	1.82682	1.82682	1.82682
	Li *et al*. (2008) (3D)	1.82682	1.82682	-	1.82682	1.82682	1.82682

Table 12 Continued

p	Theory	1-0-1	2-1-2	2-1-1	1-1-1	2-2-1	1-2-1
0.5	Present	1.44417	1.48415	1.50640	1.51927	1.54717	1.57453
	Present (FEM)	1.4394	1.4797	1.5021	1.5151	1.5431	1.5705
	Zenkour (2005b) (TSDT)	1.44424	1.48408	1.51253	1.51922	1.55199	1.57451
	Zenkour (2005b) (SSDT)	1.44436	1.48418	1.51258	1.51927	1.55202	1.57450
	Meiche *et al*. (2011) (HSDT)	1.44419	1.48405	1.50636	1.51922	1.54714	1.57458
	Bessaim *et al*. (2013) (Quasi-3D)	1.44621	1.48611	-	1.52130	1.55016	1.57670
	Li *et al*. (2008) (3D)	1.44614	1.48608	-	1.52131	1.54926	1.57668
1	Present	1.24410	1.30086	1.33397	1.35385	1.39612	1.43954
	Present (FEM)	1.2420	1.2985	1.3317	1.3513	1.3937	1.4368
	Zenkour (2005b) (TSDT)	1.24320	1.30011	1.34888	1.35333	1.40789	1.43934
	Zenkour (2005b) (SSDT)	1.24335	1.30023	1.34894	1.35339	1.40792	1.43931
	Meiche *et al*. (2011) (HSDT)	1.24310	1.30004	1.33328	1.35331	1.39559	1.43940
	Bessaim *et al*. (2013) (Quasi-3D)	1.24495	1.30195	-	1.35527	1.39987	1.44143
	Li *et al*. (2008) (3D)	1.24470	1.30181	-	1.35523	1.39763	1.44137
5	Present	0.94751	0.98289	1.03129	1.04533	1.10952	1.17412
	Present (FEM)	0.94618	0.98133	1.0301	1.0463	1.1081	1.1720
	Zenkour (2005b) (TSDT)	0.94598	0.98184	1.07432	1.04466	1.14731	1.17397
	Zenkour (2005b) (SSDT)	0.94630	0.98207	1.07445	1.04481	1.14741	1.17399
	Meiche *et al*. (2011) (HSDT)	0.94574	0.98166	1.03033	1.04455	1.10875	1.17397
	Bessaim *et al*. (2013) (Quasi-3D)	0.94716	0.98311	-	1.04613	1.11723	1.17579
	Li *et al*. (2008) (3D)	0.94476	0.98103	-	1.04532	1.10983	1.17567
10	Present	0.93024	0.94422	0.99288	0.99632	1.06172	1.12338
	Present (FEM)	0.92904	0.94278	0.99188	0.99467	1.0605	1.1214
	Zenkour (2005b) (TSDT)	0.92839	0.94297	1.03862	0.99551	1.10533	1.12314
	Zenkour (2005b) (SSDT)	0.92875	0.94332	1.04558	0.99519	1.04154	1.13460
	Meiche *et al*. (2011) (HSDT)	0.92811	0.94275	0.99184	0.99536	1.06081	1.12311
	Bessaim *et al*. (2013) (Quasi-3D)	0.92952	0.94410	-	0.99684	1.07015	1.12486
	Li *et al*. (2008) (3D)	0.92727	0.94078	-	0.99523	1.06104	1.12466

Table 13 Nondimensional fundamental frequency $\overline{\omega}$ of Al/Al_2O_3 sandwich square plates with homogeneous softcore (b/h = 10)

p	Theory	1-0-1	2-1-2	2-1-1	1-1-1	2-2-1	1-2-1
0	Present	0.92836	0.92836	0.92836	0.92836	0.92836	0.92836
	Present (FEM)	0.9273	0.9273	0.9273	0.9273	0.9273	0.9273
	Bessaim *et al*. (2013) (Quasi-3D)	0.92897	0.92897	-	0.92897	0.92897	0.92897
	Li *et al*. (2008) (3D)	0.92897	0.92897	-	0.92897	0.92897	0.92897

Table 13 Continued

p	Theory	1-0-1	2-1-2	2-1-1	1-1-1	2-2-1	1-2-1
0.5	Present	1.57228	1.52489	1.48614	1.48373	1.43528	1.41650
	Present (FEM)	1.5719	1.5243	1.4857	1.4831	1.4347	1.4158
	Bessaim *et al*. (2013) (Quasi-3D)	1.57705	1.53096	-	1.48853	1.44040	1.41788
	Li *et al*. (2008) (3D)	1.57352	1.52588	-	1.48459	1.43419	1.41662
1	Present	1.72003	1.67404	1.63014	1.63030	1.57356	1.55693
	Present (FEM)	1.7173	1.6716	1.6280	1.6281	1.5717	1.5549
	Bessaim *et al*. (2013) (Quasi-3D)	1.72814	1.68625	-	1.64199	1.58430	1.56301
	Li *et al*. (2008) (3D)	1.72227	1.67437	-	1.63053	1.57037	1.55788
5	Present	1.83900	1.82902	1.78974	1.79866	1.74266	1.73181
	Present (FEM)	1.8355	1.8259	1.7869	1.7958	1.7402	1.7294
	Bessaim *et al*. (2013) (Quasi-3D)	1.84465	1.84456	-	1.82032	1.75972	1.75143
	Li *et al*. (2008) (3D)	1.84198	1.82611	-	1.78956	1.72726	1.72670
10	Present	1.83744	1.84126	1.80581	1.81826	1.76525	1.75627
	Present (FEM)	1.8338	1.8380	1.8028	1.8153	1.7626	1.7537
	Bessaim *et al*. (2013) (Quasi-3D)	1.84113	1.85489	-	1.83973	1.78163	1.77878
	Li *et al*. (2008) (3D)	1.84020	1.83987	-	1.80813	1.74779	1.74811

Table 14 Nondimensional critical buckling loads $\overline{N}_{cr}$ of Al/Al_2O_3 sandwich square plates subjected to uniaxial compressive load ($\gamma = 0$) with homogeneous hardcore ($b/h = 10$)

p	Theory	1-0-1	2-1-2	2-1-1	1-1-1	2-2-1	1-2-1
0	Present	13.02212	13.02212	13.02212	13.02212	13.02212	13.02212
	Present (FEM)	12.9682	12.9682	12.9682	12.9682	12.9682	12.9682
	Zenkour (2005b) (TSDT)	13.00495	13.00495	13.00495	13.00495	13.00495	13.00495
	Zenkour (2005b) (SSDT)	13.00606	13.00606	13.00606	13.00606	13.00606	13.00606
	Meiche *et al*. (2011) (HSDT)	13.00552	13.00552	13.00552	13.00552	13.00552	13.00552
0.5	Present	7.36402	7.94190	8.22498	8.43730	8.81046	9.21716
	Present (FEM)	7.30884	7.88926	8.1724	8.38593	8.76012	9.16671
	Zenkour (2005b) (TSDT)	7.36437	7.94084	8.22470	8.43645	8.80997	9.21681
	Zenkour (2005b) (SSDT)	7.36568	7.94195	8.22538	8.43712	8.81037	9.21670
	Meiche *et al*. (2011) (HSDT)	7.36380	7.94046	8.22471	8.43647	8.81029	9.21757
1	Present	5.17491	5.84707	6.19951	6.46995	6.95434	7.50888
	Present (FEM)	5.15299	5.82231	6.17511	6.44260	6.92653	7.47726
	Zenkour (2005b) (TSDT)	5.16713	5.84006	6.19394	6.46474	6.94944	7.50656
	Zenkour (2005b) (SSDT)	5.16846	5.84119	6.19461	6.46539	6.94980	7.50629
	Meiche *et al*. (2011) (HSDT)	5.16629	5.83941	6.19371	6.46450	6.94952	7.50719

Table 14 Continued

p	Theory	1-0-1	2-1-2	2-1-1	1-1-1	2-2-1	1-2-1
5	Present	2.66706	3.04926	3.40832	3.58429	4.11636	4.73597
	Present (FEM)	2.65566	3.03618	3.39720	3.56894	4.10226	4.71581
	Zenkour (2005b) (TSDT)	2.65821	3.04257	3.40351	3.57956	4.11209	4.73469
	Zenkour (2005b) (SSDT)	2.66006	3.04406	3.40449	3.58063	4.11288	4.73488
	Meiche *et al*. (2011) (HSDT)	2.65679	3.04141	3.40280	3.57874	4.11157	4.73463
10	Present	2.49751	2.75383	3.09685	3.20006	3.71221	4.28184
	Present (FEM)	2.48699	2.74203	3.08704	3.18635	3.70008	4.26359
	Zenkour (2005b) (TSDT)	2.48727	2.74632	3.09190	3.19471	3.70752	4.27991
	Zenkour (2005b) (SSDT)	2.48928	2.74844	3.13443	3.19456	3.14574	4.38175
	Meiche *et al*. (2011) (HSDT)	2.48574	2.74498	3.09111	3.19373	3.70686	4.27964

Table 15 Nondimensional critical buckling loads $\overline{N}_{cr}$ of Al/Al_2O_3 sandwich square plates subjected to biaxial compressive load ($\gamma = 1$) with homogeneous hardcore ($b/h = 10$)

p	Theory	1-0-1	2-1-2	2-1-1	1-1-1	2-2-1	1-2-1
0	Present	6.51106	6.51106	6.51106	6.51106	6.51106	6.51106
	Present (FEM)	6.48413	6.48413	6.48413	6.48413	6.48413	6.48413
	Zenkour (2005b) (TSDT)	6.50248	6.50248	6.50248	6.50248	6.50248	6.50248
	Zenkour (2005b) (SSDT)	6.50303	6.50303	6.50303	6.50303	6.50303	6.50303
	Meiche *et al*. (2011) (HSDT)	6.50276	6.50276	6.50276	6.50276	6.50276	6.50276
0.5	Present	3.68201	3.97095	4.11249	4.21865	4.40523	4.60858
	Present (FEM)	3.65443	3.94464	408.623	4.19297	4.38007	4.58336
	Zenkour (2005b) (TSDT)	3.68219	3.97042	4.11235	4.21823	4.40499	4.60841
	Zenkour (2005b) (SSDT)	3.68284	3.97097	4.11269	4.21856	4.40519	4.60835
	Meiche *et al*. (2011) (HSDT)	3.68190	3.97023	4.11236	4.21823	4.40514	4.60878
1	Present	2.58746	2.92354	3.09976	3.23497	3.47717	3.75444
	Present (FEM)	2.57650	2.91116	3.08756	3.22130	3.46327	3.73864
	Zenkour (2005b) (TSDT)	2.58357	2.92003	3.09697	3.23237	3.47472	3.75328
	Zenkour (2005b) (SSDT)	2.58423	2.92060	3.09731	3.23270	3.47490	3.75314
	Meiche *et al*. (2011) (HSDT)	2.58315	2.91970	3.09686	3.23225	3.47476	3.75359
5	Present	1.33353	1.52463	1.70416	1.79214	2.05818	2.36798
	Present (FEM)	1.32783	1.51809	1.69860	1.78447	2.05113	2.35791
	Zenkour (2005b) (TSDT)	1.32910	1.52129	1.70176	1.78978	2.05605	2.36734
	Zenkour (2005b) (SSDT)	1.33003	1.52203	1.70224	1.79032	2.05644	2.36744
	Meiche *et al*. (2011) (HSDT)	1.32839	1.52071	1.70140	1.78937	2.05578	2.36731
10	Present	1.24875	1.37692	1.54843	1.60003	1.85611	2.14092
	Present (FEM)	1.24350	1.37102	1.54352	1.59318	1.85004	2.13180

Table 15 Continued

p	Theory	1-0-1	2-1-2	2-1-1	1-1-1	2-2-1	1-2-1
	Zenkour (2005b) (TSDT)	1.24363	1.37316	1.54595	1.59736	1.85376	2.13995
10	Zenkour (2005b) (SSDT)	1.24475	1.37422	1.56721	1.59728	1.57287	2.19087
	Meiche *et al*. (2011) (HSDT)	1.24287	1.37249	1.54556	1.59687	1.85343	2.13982

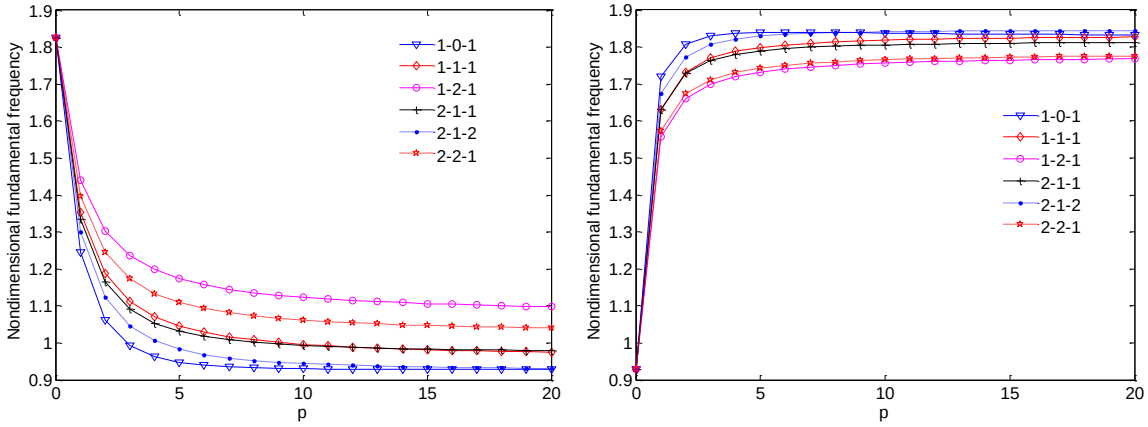

(a) Homogeneous hardcore (b) Homogeneous softcore

Fig. 6 Effect of the power-law index *p* on the nondimensional fundamental frequency ($\overline{\omega}$) of Al/Al_2O_3 sandwich square plates (*b*/*h* = 10)

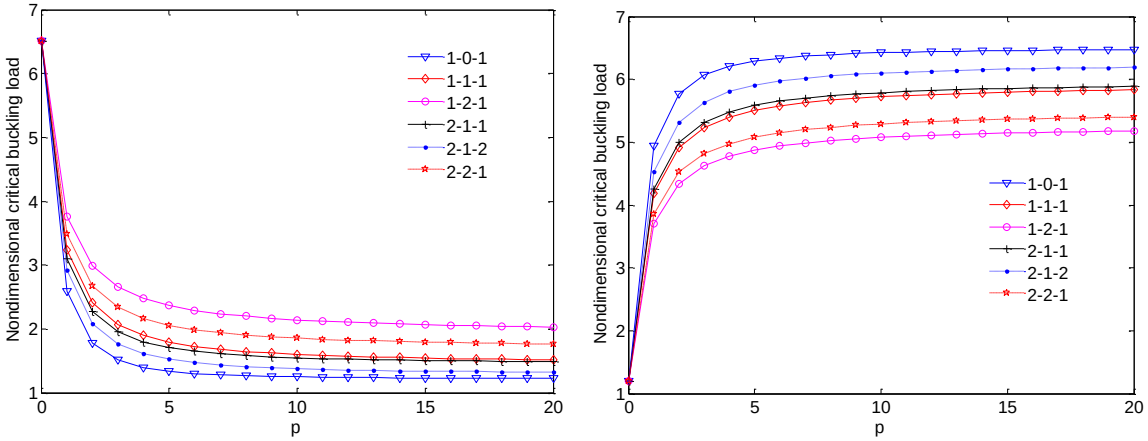

(a) Homogeneous hardcore (b) Homogeneous softcore

Fig. 7 Effect of the power-law index *p* on the nondimensional critical buckling loads ($\overline{N}_{cr}$) of Al/Al_2O_3 sandwich square plates (*b*/*h* = 10) under biaxial compressions (γ = 1)

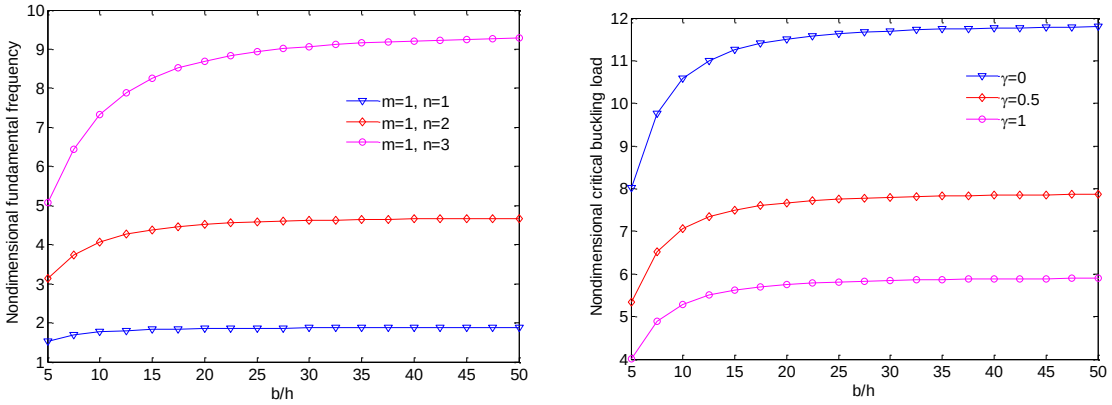

(a) Nondimensional fundamental frequency (b) Nondimensional critical buckling

Fig. 8 Effect of the side-to-thickness ratio b/h on the nondimensional fundamental frequency ($\overline{\omega}$) and critical buckling load ($\overline{N}_{cr}$) of (2-2-1) sandwich square plates with homogeneous softcore (p = 10)

Finally, the effects of the power-law index and side-to-thickness ratio on the first three natural frequencies and the critical buckling loads of (2-2-1) sandwich plate with homogeneous softcore is displayed in Figure 8. It is evident that they increase with an increase of the side-to-thickness ratio, and shear deformation effect becomes very effective in a relatively large region ($b/h \leq 40$) (Fig. 8). Three groups of curves are seen, for vibration analysis, the highest group is for the third mode (m = 1, n = 3) and the lowest group is for the first mode (m = 1, n = 1), for buckling analysis, the highest group is for the case of γ = 0 (uniaxial compression) and the lowest group is for the case of γ = 1 (biaxial compression).

4. Conclusions

A refined higher-order shear deformation theory for bending, vibration and buckling analysis of FG sandwich plates is proposed in this paper. It contains only four unknowns, accounts for a hyperbolic distribution of transverse shear stress and satisfies the traction free boundary conditions. Equations of motion are derived from Hamilton's principle. The Navier-type and finite element solutions are derived and compared with the existing solutions to verify the validity of the developed theory. Numerical results are obtained for FG sandwich plates with homogeneous hardcore and softcore to investigate the effects of the boundary conditions, power-law index, thickness ratio of layers and side-to-thickness ratio on the deflections, stresses, critical buckling load and natural frequencies. It is observed that the present theory with four unknowns predicts the response with more accuracy and less computational cost as compared with five unknowns shear deformation theories.

Acknowledgments

This research is funded by Vietnam National Foundation for Science and Technology

Development (NAFOSTED) under Grant No. 107.02-2012.07.

References

Abdelaziz, H.H., Atmane, H.A., Mechab, I., Boumia, L., Tounsi, A. and Abbas, A.B.E. (2011), "Static analysis of functionally graded sandwich plates using an efficient and simple refined theory", *Chinese J. Aeronaut.*, **24**(4), 434-448.

Baferani, A.H., Saidi, A.R. and Jomehzadeh, E. (2011), "An exact solution for free vibration of thin functionally graded rectangular plates", *P.I. Mech.. Eng. C-J Mech.*, **225**(3), 526-536.

Bessaim, A., Houari, M.S., Tounsi, A., Mahmoud, S. and Adda Bedia, E.A. (2013), "A new higher-order shear and normal deformation theory for the static and free vibration analysis of sandwich plates with functionally graded isotropic face sheets", *J. Sandw. Struct. Mater.*, 15(6), 671-703.

Chen, C.S., Chen, T.J. and Chien, R.D. (2006), "Nonlinear vibration of initially stressed functionally graded plates", *Thin-Wall. Struct.*, **44**(8), 844-851.

Chen, C., Hsu, C. and Tzou, G. (2009), "Vibration and stability of functionally graded plates based on a higher-order deformation theory", *J. Reinf. Plast. Comp.*, **28**(10), 1215-1234.

Croce, L.D. and Venini, P. (2004), "Finite elements for functionally graded Reissner-Mindlin plates", *Comput. Method. Appl. M.*, **193**(9-11), 705-725.

Efraim, E. and Eisenberger, M. (2007), "Exact vibration analysis of variable thickness thick annular isotropic and FGM plates", *J. Sound Vib.*, **299**(4-5), 720-738.

Feldman, E. and Aboudi, J. (1997), "Buckling analysis of functionally graded plates subjected to uniaxial loading", *Compos. Struct.*, **38**(1-4), 29-36.

Gilhooley, D.F., Batra, R.C., Xiao, J.R., McCarthy, M.A., Gillespie, Jr. J.W. (2007), "Analysis of thick functionally graded plates by using higher-order shear and normal deformable plate theory and MLPG method with radial basis functions", *Compos. Struct.*, **80**(4), 539-552.

Grover, N., Maiti, D. and Singh, B. (2013), "A new inverse hyperbolic shear deformation theory for static and buckling analysis of laminated composite and sandwich plates", *Compos. Struct.*, **95**, 667-675.

Hamidi, A., Zidi, M., Houari, M.S.A. and Tounsi, A. (2012), "A new four variable refined plate theory for bending response of functionally graded sandwich plates under thermomechanical loading", *Compos. Part B: Eng.* [In Press]

Hosseini-Hashemi, S., Fadaee, M. and Atashipour, S.R. (2011), "A new exact analytical approach for free vibration of Reissner-Mindlin functionally graded rectangular plates", *Int. J. Mech. Sci.*, **53**(1), 11-22.

Javaheri, R. and Eslami, M. (2002), "Buckling of functionally graded plates under in-plane compressive loading", *J. Appl. Math. Mech.*, **82**(4), 277-283.

Jha, D.K., Kant, T. and Singh, R.K. (2013), "Free vibration response of functionally graded thick plates with shear and normal deformations effects", *Compos. Struct.*, **96**, 799-823.

Lee, Y.Y., Zhao, X. and Liew, K.M. (2009), "Thermoelastic analysis of functionally graded plates using the element-free kp-Ritz method", *Smart Mater. Struct.*, **18**(3), 035007.

Li, Q., Iu, V.P. and Kou, K.P. (2008), "Three-dimensional vibration analysis of functionally graded material sandwich plates", *J. Sound Vib.*, **311**(1-2), 498-515.

Mahdavian, M. (2009), "Buckling analysis of simply-supported functionally graded rectangular plates under non-uniform in-plane compressive loading", *J. Solid Mech.*, **1**(3), 213-225.

Mantari, J.L. and Soares, C.G. (2012), "Generalized hybrid quasi-3D shear deformation theory for the static analysis of advanced composite plates", *Compos. Struct.*, **94**(8), 2561-2575.

Mantari, J.L. and Soares, C.G. (2013), "A novel higher-order shear deformation theory with stretching effect for functionally graded plates", *Compos. Part B: Eng.*, **45**(1), 268-281.

Matsunaga, H. (2008), "Free vibration and stability of functionally graded plates according to a 2-D higher-order deformation theory", *Compos. Struct.*, **82**(4), 499-512.

Meiche, N.E., Tounsi, A., Ziane, N., Mechab, I., Adda.Bedia, E.A. (2011), "A new hyperbolic shear deformation theory for buckling and vibration of functionally graded sandwich plate", *Int. J. Mech. Sci.*,

53(4), 237-247.
Mohammadi, M., Saidi, A. and Jomehzadeh, E. (2010), "Levy solution for buckling analysis of functionally graded rectangular plates", *Appl. Compos. Mater.*, **17**(2), 81-93.
Naderi, A. and Saidi, A. (2010), "On pre-buckling configuration of functionally graded Mindlin rectangular plates", *Mech. Res. Commun.*, **37**(6), 535-538.
Neves, A.M.A., Ferreira, A.J.M., Carrera, E., Cinefra, M., Roque, C.M.C., Jorge, R.M.N. and Soares, C.M.M. (2012a), "A quasi-3D hyperbolic shear deformation theory for the static and free vibration analysis of functionally graded plates", *Compos. Struct.*, **94**(5), 1814-1825.
Neves, A.M.A., Ferreira, A.J.M., Carrera, E., Roque, C.M.C., Cinefra, M., Jorge, R.M.N. and Soares, C.M.M. (2012b), "A quasi-3D sinusoidal shear deformation theory for the static and free vibration analysis of functionally graded plates", *Compos. Part B: Eng.*, **43**(2), 711-725.
Neves, A.M.A., Ferreira, A.J.M., Carrera, E., Cinefra, M., Jorge, R.M.N. and Soares, C.M.M. (2012c), "Static analysis of functionally graded sandwich plates according to a hyperbolic theory considering Zig-Zag and warping effects", *Adv. Eng. Softw.*, **52**, 30-43.
Neves, A.M.A., Ferreira, A.J.M., Carrera, E., Cinefra, M., Roque, C.M.C., Jorge, R.M.N. and Soares, C.M.M. (2013), "Static, free vibration and buckling analysis of isotropic and sandwich functionally graded plates using a quasi-3D higher-order shear deformation theory and a meshless technique", *Compos. Part B: Eng.*, **44**(1), 657-674.
Nguyen-Xuan, H., Tran, L.V., Thai, C.H. and Nguyen-Thoi, T. (2012), "Analysis of functionally graded plates by an efficient finite element method with node-based strain smoothing", *Thin-Wall. Struct.*, **54**, 1-18.
Pradyumna, S. and Bandyopadhyay, J.N. (2008), "Free vibration analysis of functionally graded curved panels using a higher-order finite element formulation", *J. Sound Vib.*, **318**(1-2), 176-192.
Reddy, J.N. (2000), "Analysis of functionally graded plates", *Int. J. Numer. Method. Eng.*, **47**(1-3), 663-684.
Sobhy, M. (2013), "Buckling and free vibration of exponentially graded sandwich plates resting on elastic foundations under various boundary conditions", *Compos. Struct.*, **99**, 76-87.
Talha, M. and Singh, B.N. (2010), "Static response and free vibration analysis of FGM plates using higher order shear deformation theory", *Appl. Math. Model.*, **34**(12), 3991-4011.
Thai, H.T. and Choi, D.H. (2013a), "A simple first-order shear deformation theory for the bending and free vibration analysis of functionally graded plates", *Compos. Struct.*, **101**, 332-340.
Thai, H.T. and Choi, D.H. (2013b), "Finite element formulation of various four unknown shear deformation theories for functionally graded plates", *Finite Elem. Anal. Des.*, **75**, 50-61.
Thai, H.-T. and Kim, S.-E. (2013), "A simple quasi-3D sinusoidal shear deformation theory for functionally graded plates", *Compos. Struct.*, **99**, 172-180.
Thai, H.-T., Nguyen, T.-K., Vo, T.P. and Lee, J. (2014), "Analysis of functionally graded sandwich plates using a new first-order shear deformation theory", *Eur. J. Mech. A/Solids*, **45**, 211-225.
Xiang, S., Jin, Y., Bi, Z., Jiang, S. and Yang, M.S. (2011), "A *n*-order shear deformation theory for free vibration of functionally graded and composite sandwich plates", *Compos. Struct.*, **93**(11), 2826-2832.
Zenkour, A.M. (2005a), "A comprehensive analysis of functionally graded sandwich plates: Part 1 - Deflection and stresses", *Int. J. Solids Struct.*, **42**(18-19), 5224-5242.
Zenkour, A.M. (2005b), "A comprehensive analysis of functionally graded sandwich plates: Part 2 - Buckling and free vibration", *Int. J. Solids Struct.*, **42**(18-19), 5243-5258.
Zenkour, A.M. (2006), "Generalized shear deformation theory for bending analysis of functionally graded materials", *Appl. Math. Model.*, **30**(1), 67-84.
Zenkour, A.M. (2013a), "Bending analysis of functionally graded sandwich plates using a simple four-unknown shear and normal deformations theory", *J. Sandw. Struct. Mater.* DOI: 10.1177/1099636213498886
Zenkour, A.M. (2013b), "A simple four-unknown refined theory for bending analysis of functionally graded plates", *Appl. Math. Model.*, **37**(20-21), 9041-9051.
Zhao, X., Lee, Y.Y. and Liew, K.M. (2009a), "Mechanical and thermal buckling analysis of functionally graded plates", *Compos. Struct.*, **90**(2), 161-171.

Zhao, X., Lee, Y.Y. and Liew, K.M. (2009b), "Free vibration analysis of functionally graded plates using the element-free kp-Ritz method", *J. Sound Vib.*, **319**(3-5), 918-939.

BU